2wp mix

X-582-74-41
PREPRINT

NASA TM X- 70591

SOLUTION OF AN EIGENVALUE PROBLEM FOR THE LAPLACE OPERATOR ON A SPHERICAL SURFACE

HARVEY WALDEN

FEBRUARY 1974

GSFC — GODDARD SPACE FLIGHT CENTER —
GREENBELT, MARYLAND

80

X-582-74-41

SOLUTION OF AN EIGENVALUE PROBLEM FOR THE LAPLACE OPERATOR ON A SPHERICAL SURFACE

by
Harvey Walden

February 1974

NATIONAL AERONAUTICS AND SPACE ADMINISTRATION
GODDARD SPACE FLIGHT CENTER
Greenbelt, Maryland

SOLUTION OF AN EIGENVALUE PROBLEM FOR THE LAPLACE OPERATOR ON A SPHERICAL SURFACE

Harvey Walden

ABSTRACT

Methods for obtaining approximate solutions for the fundamental eigenvalue of the Laplace-Beltrami operator (also referred to as the membrane eigenvalue problem for the vibration equation) on the unit spherical surface are developed. Two specific types of spherical surface domains are considered: (1) the interior of a spherical triangle, i.e., the region bounded by arcs of three great circles, and (2) the exterior of a great circle arc extending for less than π radians on the sphere (a spherical surface with a slit). In both cases, zero boundary conditions are imposed. In order to solve the resulting second-order elliptic partial differential equations in two independent variables, a finite difference approximation is derived. The symmetric (generally five-point) finite difference equations that develop are written in matrix form and then solved by the iterative method of point successive overrelaxation. Upon convergence of this iterative method, the fundamental eigenvalue is approximated by iteration utilizing the power method as applied to the finite Rayleigh quotient. The implementation of these numerical techniques is described in detail, including the presentation of separate algorithms for calculating the fundamental eigenvalue for the two distinct domains considered. Although analytical solutions to this eigenvalue problem are not available in the general case, the problem is solved analytically for

exact values of the fundamental eigenvalue for certain special cases. These exact solutions are useful in providing checks on the numerical results presented based upon digital computer calculations. Several tables of numerical applications for various cases of interest are displayed and discussed.

ACKNOWLEDGMENTS

The research studies contained in this report were presented and submitted in December 1973 as a thesis to the faculty of the Graduate School of the University of Maryland at College Park in partial fulfillment of the requirements for the degree of Master of Arts in mathematics. The author wishes to express his sincere appreciation to Professor R. Bruce Kellogg of the Institute for Fluid Dynamics and Applied Mathematics at the University of Maryland for his interest in and direction of the research efforts described herein and for his guidance and painstaking review throughout the writing of this paper.

TABLE OF CONTENTS

LIST OF TABLES

LIST OF FIGURES

SECTION I

INTRODUCTION

Let G be a polyhedron in Euclidean three-dimensional space whose boundary is denoted by ∂G. Consider the problem:

$$\begin{aligned} \Delta v &= f \quad \text{in } G, \\ v &= 0 \quad \text{on } \partial G, \end{aligned} \tag{1}$$

where Δ denotes the Laplacian and v and f are defined in G. It is known (Reference 1) that the derivatives of v may become singular near a vertex of G, and the severity of the singularity is determined by the fundamental eigenvalue of an associated eigenvalue problem for the Laplace-Beltrami operator on the unit sphere. Methods for obtaining approximate solutions of this associated eigenvalue problem will be considered in this paper.

If spherical co-ordinates are introduced such that

$$\begin{aligned} x &= r \sin\phi \cos\theta, \\ y &= r \sin\phi \sin\theta, \\ z &= r \cos\phi, \end{aligned} \tag{2}$$

then the Laplacian may be written (Reference 2, p. 225)

$$\Delta u = r^{-2}(r^2 u_r)_r + r^{-2}\Lambda u, \tag{3}$$

where

$$\Lambda u = \csc\phi[(u_\theta \csc\phi)_\theta + (u_\phi \sin\phi)_\phi], \tag{4}$$

and where the subscript notation is used to indicate partial differentiation. If the origin of the co-ordinate system is placed at a vertex of G, then the singularity in the solution of problem (1) at the origin is related to the eigenvalue problem

$$\begin{aligned} \Lambda u + \lambda u &= 0 \quad \text{in } D, \\ u &= 0 \quad \text{on } \partial D, \end{aligned} \tag{5}$$

where D represents the area on the surface of a small sphere (centered at the origin) and bounded by the polyhedron G. In this paper, the case in which the region D is a spherical triangle T, i.e., the region bounded by three great circles, will be considered. Also to be discussed is the case in which D is a slit domain, consisting of the exterior of an arc of a great circle on the sphere.

Without loss of generality, it may be assumed that the sphere is of unit radius, so that the spherical co-ordinates satisfy

$$\begin{aligned} r &= 1, \\ 0 &\le \phi \le \pi, \\ 0 &\le \theta < 2\pi. \end{aligned} \tag{6}$$

The boundary ∂D will consist of arcs of three great circles on the unit sphere. The spherical co-ordinate system is defined so that the origin of co-ordinates is at the center of the sphere, the z-axis intersects the unit sphere at a vertex of T (i.e., at an intersection point of two of the great circles specifying T), and the x, z-plane contains a side of T which is less than π radians in length. In this manner, the relevant arcs of the three great circles specifying T are given by

$$\theta = 0, \tag{7a}$$

$$\theta = \Theta, \tag{7b}$$

$$z = ax + by, \tag{7c}$$

where Θ, a, and b are all constants (see Figure 1). Equation (7c) may be transformed to spherical co-ordinates by use of equations (2) as

$$\cot \phi = a \cos \theta + b \sin \theta. \tag{8}$$

Equations (7a), (7b), and (8) may be regarded as defining two domains on the sphere, the region $R(\Theta, a, b)$ given by the inequalities

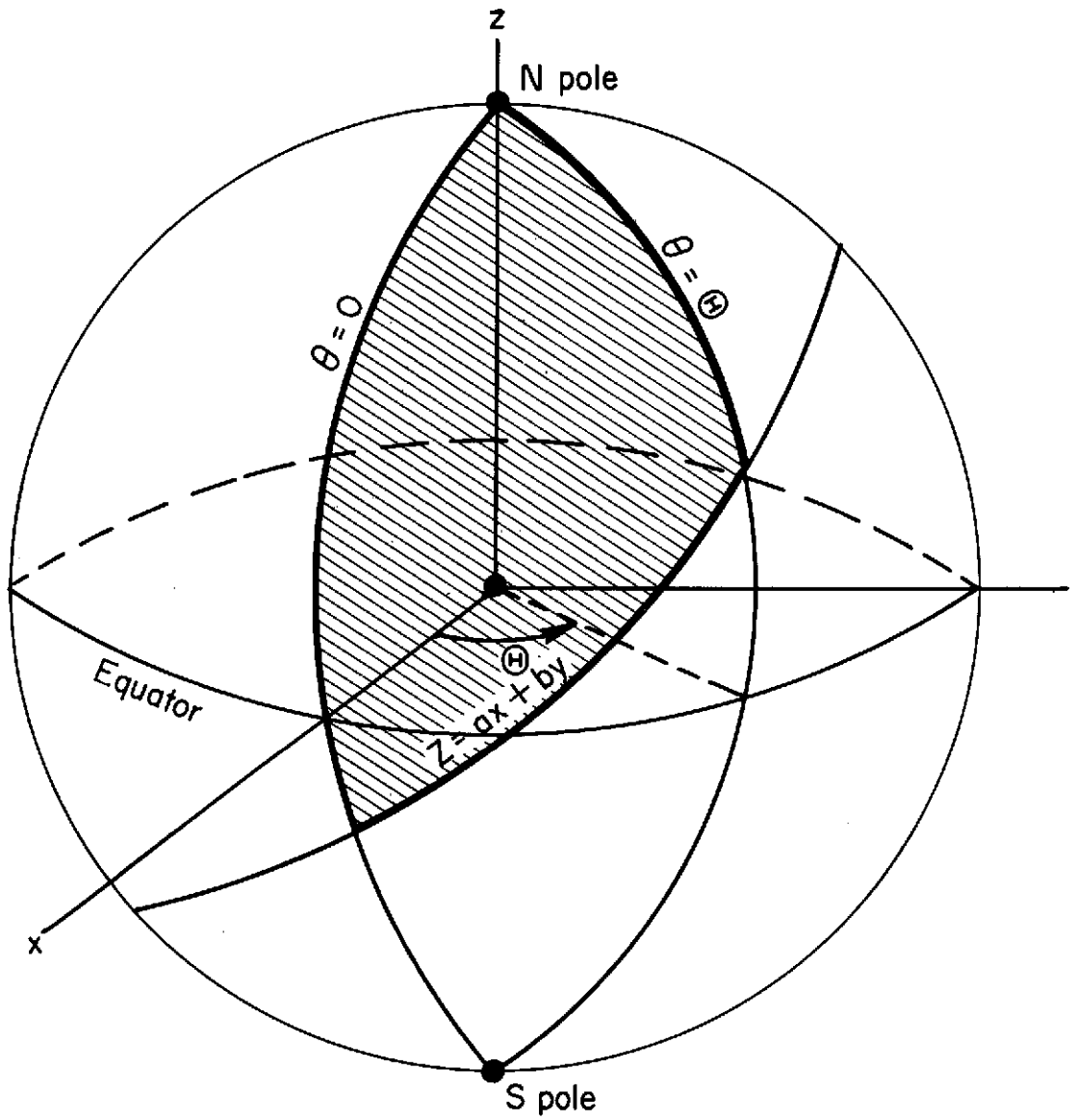

Figure 1. The spherical triangle T bounded by arcs of three great circles (the interior R of T is shown shaded), which are specified by the three parameters Θ, a, and b

$$0 < \theta < \Theta,$$
$$\cot \phi > a \cos \theta + b \sin \theta, \tag{9}$$

and the region $S(\Theta, a, b)$ complementary to $R(\Theta, a, b)$. Both the interior R and the exterior S of the spherical triangle T are thus specified by the three parameters Θ, a, and b, which satisfy the inequalities

$$0 \leq \Theta < 2\pi,$$
$$-\infty < a, b < \infty. \tag{10}$$

The eigenvalue problem (5) for the unit sphere may be written, by virtue of equation (4), as

$$(u_\theta \csc \phi)_\theta + (u_\phi \sin \phi)_\phi + \lambda u \sin \phi = 0 \text{ in D}, \tag{11a}$$

$$u = 0 \text{ on } \partial D, \tag{11b}$$

where D is one of the regions $R(\Theta, a, b)$ or $S(\Theta, a, b)$. Equation (11a) may be expanded as

$$u_{\theta\theta} \csc \phi + (u_\phi \sin \phi)_\phi + \lambda u \sin \phi = 0. \tag{12}$$

It is well known (Reference 2, p. 298) that the eigenvalue problem (5) has a denumerably infinite sequence of positive eigenvalues which may be ordered so that

$$0 < \lambda_1 < \lambda_2 \leq \lambda_3 \leq \ldots\ldots,$$

as well as a corresponding sequence of linearly independent eigenfunctions u_1, $u_2, \ldots$ The smallest positive eigenvalue λ_1 for this problem is known as the fundamental eigenvalue. In this paper, the fundamental eigenvalue of equation (12) will be determined for the following two cases: (1) when D is the interior R of a spherical triangle, and (2) when D is the exterior S of a spherical "triangle" which has degenerated to a line in the special situation: $\Theta = 0$. In both cases, the boundary condition (11b) applies. In order to solve the

second-order elliptic partial differential equation (12) in two independent variables θ, ϕ, a finite difference approximation is derived. The resulting finite difference equations are written in matrix form and then solved by the iterative method of point successive overrelaxation. Upon convergence of this iterative method, the fundamental eigenvalue is found by iteration utilizing the power method as applied to the finite Rayleigh quotient. Numerical results for a number of cases are presented and then discussed.

SECTION II

FINITE DIFFERENCE APPROXIMATION

In the following, the domain D on the spherical surface is taken to be the interior $R(\Theta, a, b)$ of a spherical triangle, with $0 < \Theta < 2\pi$. Then the two-dimensional spherical surface may be mapped directly onto the θ,ϕ-plane in the manner that cartographers would refer to as Mercator's projection in the case of the Earth's surface. The spherical wedge-shaped surface bounded by the meridional arcs $\theta = 0, \Theta$ is thus mapped into the plane rectangle bounded by the two pairs of parallel lines, $\theta = 0, \Theta$ and $\phi = 0, \pi$. The arc of the great circle forming the third side of the spherical triangle, specified by equation (8), is mapped into a continuous curve extending from the ordinate axis $\theta = 0$ to the parallel side of the rectangular region, $\theta = \pi$, and lying wholly within the rectangular closed region (see Figure 2).

In problems involving elliptic partial differential equations for which an analytic solution is not known, such as equation (11), the method of finite differences is most commonly employed to determine numerical results. This finite-difference technique involves first establishing a network of grid points throughout the rectangular region of interest occupied by the independent variables θ and ϕ. Suppose, for the moment, that positive constant grid spacings of h_θ and h_ϕ are chosen in the θ- and ϕ-directions, respectively. Then the rectangular network consists of the grid points

$$(\theta_i, \phi_j) = (ih_\theta, jh_\phi), \qquad \begin{matrix} i = 0, 1, 2, \ldots, N_\theta; \\ j = 0, 1, 2, \ldots, N_\phi. \end{matrix} \tag{13}$$

Here the positive integers N_θ, N_ϕ represent the number of grid intervals (or grid points less one) in the θ- and ϕ-directions, respectively, so that

$$h_\theta N_\theta = \Theta, \tag{14a}$$

$$h_\phi N_\phi = \pi. \tag{14b}$$

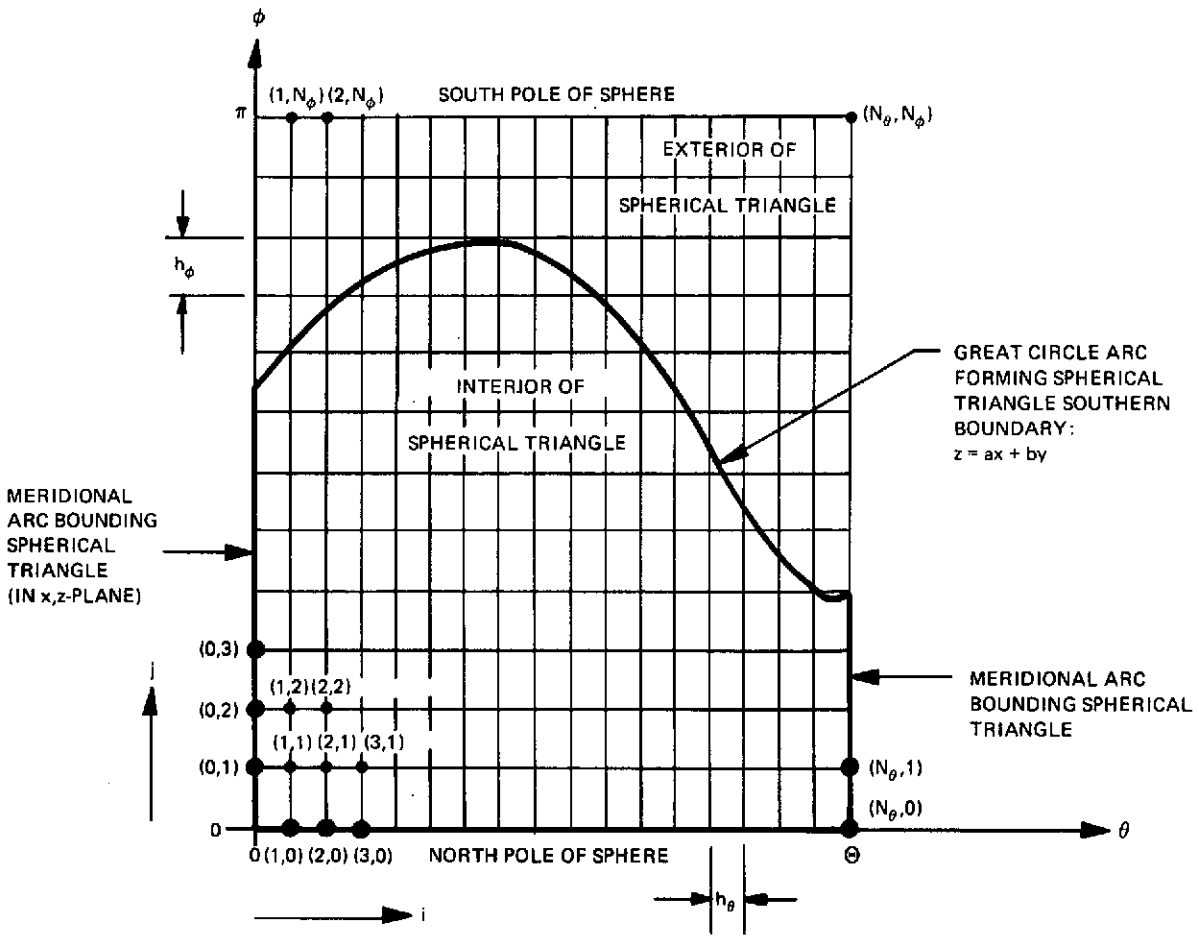

Figure 2. Network of grid points θ_i , ϕ_j superposed over the spherical wedge-shaped surface containing the spherical triangle mapped onto a plane rectangular region

In this manner, the continuous problem (11) is discretized by the replacement of the connected open domain R of the independent variables θ, ϕ with a finite set of grid points θ_i, ϕ_j (see Figure 2). If the exact solution to the partial differential equation (12) is denoted $u = u(\theta, \phi)$, then let its approximation, to be determined at each grid point by the method of finite differences, be $U = U(\theta_i, \phi_j) = U_{i,j}$. The partial derivatives involved in equation (12) will then be approximated by suitable finite-difference expressions involving h_θ, h_ϕ and $U_{i,j}$. This procedure leads to a finite system of simultaneous algebraic equations in the $U_{i,j}$, whose values may then be determined.

In order to approximate the second-order partial derivative in the first term of equation (12), use is made of the centered second difference quotient,

$$u_{\theta\theta} \cong \frac{1}{h_\theta^2} (U_{i+1,j} - 2U_{i,j} + U_{i-1,j}), \tag{15}$$

which has an error of order h_θ^2. Formula (15) arises by performing a Taylor's series expansion about the central value $U_{i,j}$ (Reference 3, pp. 430-431). In considering partial derivatives in the ϕ-direction, the nature of the singularity at the north pole, where two boundaries of the spherical triangle meet at a point with a discontinuous tangent (i.e., a corner), must be taken into account. For this reason, variable grid spacing in the ϕ-direction is introduced. Define

$$h_{\phi,j} = \phi_j - \phi_{j-1} > 0, \qquad j = 1, 2, \ldots\ldots, N_\phi \tag{16}$$

as the variable grid spacing parameter in the ϕ-direction. Then equations (13) and (14b) are seen to hold only for the case of constant grid spacing in the ϕ-direction. Now further define the midway (or averaged) grid points,

$$\left.\begin{aligned} \phi_{j+1/2} &= \frac{1}{2}(\phi_j + \phi_{j+1}) \\ \phi_{j-1/2} &= \frac{1}{2}(\phi_j + \phi_{j-1}) \end{aligned}\right\} j = 1, 2, \ldots\ldots, N_\phi - 1. \tag{17}$$

With these further definitions, the arrangement of grid points is as shown in Figure 3. The first-order partial derivative appearing in the second term of equation (12) may now be approximated by a centered midway first difference quotient,

$$(u_\phi \sin\phi)_\phi \cong \frac{(u_\phi)_{i,j+1/2} \sin\phi_{j+1/2} - (u_\phi)_{i,j-1/2} \sin\phi_{j-1/2}}{\frac{1}{2}(h_{\phi,j+1} + h_{\phi,j})} \tag{18}$$

In equation (18), the error is of order $h_{\phi,j}$, and in order to approximate the terms involving u_ϕ, a centered first difference quotient is employed:

$$(u_\phi)_{i,j+1/2} \cong \frac{U_{i,j+1} - U_{i,j}}{h_{\phi,j+1}},$$

$$(u_\phi)_{i,j-1/2} \cong \frac{U_{i,j} - U_{i,j-1}}{h_{\phi,j}}. \tag{19}$$

Combining equations (18) and (19) results in the approximation,

$$(u_\phi \sin\phi)_\phi \cong \frac{2\sin\phi_{j+1/2}}{h_{\phi,j+1} + h_{\phi,j}} \cdot \frac{U_{i,j+1} - U_{i,j}}{h_{\phi,j+1}} - \frac{2\sin\phi_{j-1/2}}{h_{\phi,j+1} + h_{\phi,j}} \cdot \frac{U_{i,j} - U_{i,j-1}}{h_{\phi,j}}. \tag{20}$$

The finite difference approximation to equation (12) may now be written, by use of equations (15) and (20), as

$$(U_{i+1,j} - 2U_{i,j} + U_{i-1,j}) \frac{\csc\phi_j}{h_\theta^2} + \frac{2\sin\phi_{j+1/2}}{h_{\phi,j+1} + h_{\phi,j}} \left(\frac{U_{i,j+1} - U_{i,j}}{h_{\phi,j+1}}\right) - \frac{2\sin\phi_{j-1/2}}{h_{\phi,j+1} + h_{\phi,j}} \left(\frac{U_{i,j} - U_{i,j-1}}{h_{\phi,j}}\right) + \lambda U_{i,j} \sin\phi_j = 0. \tag{21}$$

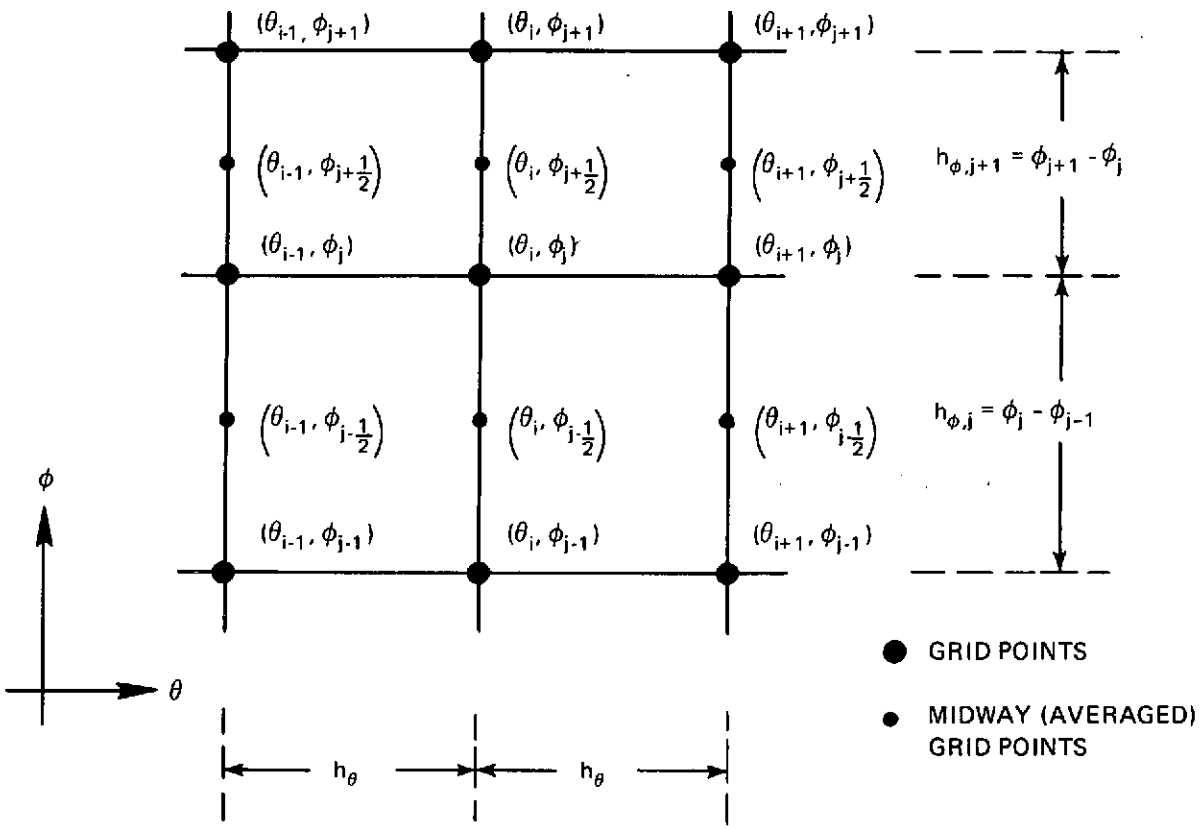

Figure 3. Arrangement of grid points with grid spacing parameters indicated

Multiplying equation (21) by the factor $(h_{\phi, j+1} + h_{\phi, j})$ and re-arranging terms yields a symmetric five-point difference equation of the form:

$$a_j U_{i,j} - b_j U_{i+1,j} - c_j U_{i,j+1} - b_j U_{i-1,j} - c_{j-1} U_{i,j-1} = \lambda e_j U_{i,j}, \tag{22}$$

where

$$b_j = \frac{\csc \phi_j}{h_\theta^2} (h_{\phi, j+1} + h_{\phi, j}), \tag{23a}$$

$$c_j = \frac{2 \sin \phi_{j+1/2}}{h_{\phi, j+1}}, \tag{23b}$$

$$e_j = (h_{\phi, j+1} + h_{\phi, j}) \sin \phi_j, \tag{23c}$$

and

$$a_j = 2b_j + c_j + c_{j-1}. \tag{23d}$$

In terms of grid points in the ϕ-direction, by virtue of equations (16) and (17),

$$b_j = \frac{\phi_{j+1} - \phi_{j-1}}{h_\theta^2 \sin \phi_j} > 0, \tag{24a}$$

$$c_j = \frac{2 \sin \frac{1}{2}(\phi_j + \phi_{j+1})}{\phi_{j+1} - \phi_j} > 0, \tag{24b}$$

and

$$e_j = (\phi_{j+1} - \phi_{j-1}) \sin \phi_j > 0. \tag{24c}$$

It is to be noted that equations (24a) and (24c) hold for $j = 1,2, \ldots, N_\phi - 1$, while equation (24b) holds for the less restrictive range, $j = 0, 1, 2, \ldots, N_\phi - 1$. In this way, equation (23d) also is valid for $j = 1, 2, \ldots, N_\phi - 1$. The finite difference equation (22) is an approximation to the continuous partial differential equation (12), which is valid for the interior R of the spherical triangle. Thus,

equation (22) holds for all rectangular interior grid points, $i = 1, 2, \ldots, N_\theta - 1$; $j = 1, 2, \ldots, N_\phi - 1$. (Grid points exterior to the spherical triangle southern boundary arc will be taken into account in the following discussion.)

The boundary conditions (11b) must be imposed on the discretized version (22) of the eigenvalue equation. With reference to Figure 2, it is seen that

$$\left.\begin{aligned} U_{0,j} &= 0 \\ U_{N_\theta,j} &= 0 \end{aligned}\right\} \quad \text{for } j = 0, 1, 2, \ldots, N_\phi, \tag{25}$$

along the meridional boundaries (7a) and (7b), respectively, and $U_{i,j} = 0$ for those grid points (i,j) such that

$$\cot \phi_j \leq a \cos \theta_i + b \sin \theta_i. \tag{26}$$

In the relation (26), equality occurs for grid points that coincide with the arc of the great circle forming the southern boundary (8) of the spherical triangle, while inequality occurs for grid points in the exterior of the triangle. Furthermore,

$$\left.\begin{aligned} U_{i,0} &= 0 \\ U_{i,N_\phi} &= 0 \end{aligned}\right\} \quad \text{for } i = 0, 1, 2, \ldots, N_\theta \tag{27}$$

at the north and south poles of the sphere, respectively, since the former lies on the boundary of the spherical triangle and the latter in the exterior of the triangle. In the limiting cases of $a, b \to -\infty$ (either or both), the triangle boundary, according to equation (8), includes the point $\phi = \pi$, the south pole, and the boundary condition (27) is still valid.

Variable grid spacing was adopted in equation (16) for the ϕ-direction in order to allow for the effect of the singularity at $\phi = 0$, the north pole. In accord with this choice, grid points in the ϕ-direction are specified by

$$\phi_j = \begin{cases} \left(\frac{2j}{N_\phi}\right)^\gamma \frac{\pi}{2} & \text{for } j = 0, 1, 2, \ldots, \frac{1}{2}N_\phi; \\ \pi - \phi_{N_\phi - j} & \text{for } j = \frac{1}{2}N_\phi + 1, \frac{1}{2}N_\phi + 2, \ldots, N_\phi, \end{cases} \tag{28}$$

where N_ϕ is assumed to be an even integer and γ is a positive constant parameter which defines the ϕ-grid spacing. If $\gamma = 1$, then formula (28) reduces to a uniform grid spacing in the ϕ-direction, as specified in the network formulas (13) and (14b) and for which the integer N_ϕ need not be even. If $\gamma > 1$, the density of grid points increases toward the poles, $\phi_0 = 0$ and $\phi_{N_\phi} = \pi$, and decreases toward the equator, $\phi_{N_\phi/2} = \pi/2$. Conversely, if $\gamma < 1$, then the density of grid points increases toward the center and decreases toward the poles. For all γ, formula (28) specifies grid points in the ϕ-direction which are symmetrically placed about the center point or equator.

SECTION III

ITERATIVE SOLUTION BY SUCCESSIVE OVERRELAXATION

In order to apply the iterative method of solution by point successive overrelaxation to the finite difference equation (22), it is advantageous to adopt a matrix formulation of the problem. Let U represent the ordered set of unknown values $U_{i,j}$ written as a vector of $(N_\theta - 1)(N_\phi - 1)$ components defined on the network of rectangular interior grid points (θ_i, ϕ_j), $i = 1, 2, 3, \ldots, N_\theta - 1$; $j = 1, 2, 3, \ldots, N_\phi - 1$. Then the finite difference equation (22), with the boundary conditions (25), (26), and (27) included, may be written in matrix form as

$$AU = \lambda EU, \tag{29}$$

where A and E are square matrices of order $(N_\theta - 1)(N_\phi - 1)$.

An example of this matrix formulation for the special case of $N_\theta = 4$, $N_\phi = 6$ appears in Figure 4. The vector U has a component associated with each rectangular interior grid point, and these components are numbered by a so-called natural ordering of the grid points (Reference 4, p. 187; Reference 5, p. 454) in which successive horizontal grid lines (see Figure 2) are scanned in order of increasing i index with the j index increasing on each new line, rectangular boundary grid points excluded. In this way, the r^{th} component of U is associated with the grid point (θ_i, ϕ_j) such that $r = i + (j - 1)(N_\theta - 1)$.

In general, the matrix A will be sparse, with the non-zero elements a_j along the principal diagonal, $-b_j$ along the two adjacent diagonals (with zeroes interspersed along these adjacent diagonals), and $-c_j$ along two other diagonals symmetrically removed from the principal diagonal by $(N_\theta - 1)$ elements, the number of rectangular interior grid points along a horizontal grid line. Since a_j, b_j, and c_j are all positive, by equations (23d) and (24), A consists of positive diagonal entries and non-positive off-diagonal entries. Furthermore, it is

$$
A = \left[\begin{array}{ccc:ccc:ccc:ccc:ccc}
a_1 & -b_1 & 0 & -c_1 & 0 & 0 & 0 & 0 & 0 & 0 & 0 & 0 & 0 & 0 & 0 \\
-b_1 & a_1 & -b_1 & 0 & -c_1 & 0 & 0 & 0 & 0 & 0 & 0 & 0 & 0 & 0 & 0 \\
0 & -b_1 & a_1 & 0 & 0 & -c_1 & 0 & 0 & 0 & 0 & 0 & 0 & 0 & 0 & 0 \\
\hdashline
-c_1 & 0 & 0 & a_2 & -b_2 & 0 & -c_2 & 0 & 0 & 0 & 0 & 0 & 0 & 0 & 0 \\
0 & -c_1 & 0 & -b_2 & a_2 & -b_2 & 0 & -c_2 & 0 & 0 & 0 & 0 & 0 & 0 & 0 \\
0 & 0 & -c_1 & 0 & -b_2 & a_2 & 0 & 0 & -c_2 & 0 & 0 & 0 & 0 & 0 & 0 \\
\hdashline
0 & 0 & 0 & -c_2 & 0 & 0 & a_3 & -b_3 & 0 & -c_3 & 0 & 0 & 0 & 0 & 0 \\
0 & 0 & 0 & 0 & -c_2 & 0 & -b_3 & a_3 & -b_3 & 0 & -c_3 & 0 & 0 & 0 & 0 \\
0 & 0 & 0 & 0 & 0 & -c_2 & 0 & -b_3 & a_3 & 0 & 0 & -c_3 & 0 & 0 & 0 \\
\hdashline
0 & 0 & 0 & 0 & 0 & 0 & -c_3 & 0 & 0 & a_4 & -b_4 & 0 & -c_4 & 0 & 0 \\
0 & 0 & 0 & 0 & 0 & 0 & 0 & -c_3 & 0 & -b_4 & a_4 & -b_4 & 0 & -c_4 & 0 \\
0 & 0 & 0 & 0 & 0 & 0 & 0 & 0 & -c_3 & 0 & -b_4 & a_4 & 0 & 0 & -c_4 \\
\hdashline
0 & 0 & 0 & 0 & 0 & 0 & 0 & 0 & 0 & -c_4 & 0 & 0 & a_5 & -b_5 & 0 \\
0 & 0 & 0 & 0 & 0 & 0 & 0 & 0 & 0 & 0 & -c_4 & 0 & -b_5 & a_5 & -b_5 \\
0 & 0 & 0 & 0 & 0 & 0 & 0 & 0 & 0 & 0 & 0 & -c_4 & 0 & -b_5 & a_5
\end{array}\right]
$$

$$
U = [U_{11}U_{21}U_{31}U_{12}U_{22}U_{32}U_{13}U_{23}U_{33}U_{14}U_{24}U_{34}U_{15}U_{25}U_{35}]^T
$$

$$
E = \mathrm{diag}[e_1\, e_1 e_1 e_2 e_2 e_2 e_3 e_3 e_3 e_4 e_4 e_4 e_5 e_5 e_5]
$$

Figure 4. The square matrix A of order $(N_\theta - 1)(N_\phi - 1) = 15$ with tridiagonal and diagonal submatrices indicated, the vector U of 15 components (the superscript "T" indicates transpose), and the square diagonal matrix E of order 15 for the special case $N_\theta = 4$, $N_\phi = 6$

seen that A is a symmetric matrix. There is a partitioning of A, as indicated in Figure 4, which results in the following block tridiagonal form:

$$A = \begin{bmatrix} A_1 & C_1 & & & & \\ C_1 & A_2 & C_2 & & & \\ & C_2 & A_3 & C_3 & & \\ & & \ddots & \ddots & \ddots & \\ & & & C_{N_\phi-2} & A_{N_\phi-1} & \end{bmatrix} \qquad (30)$$

The partitioning of A in this manner results from placing all rectangular interior grid points along a particular horizontal grid line into a block. In equation (30), each square diagonal submatrix A_j, $j = 1, 2, \ldots, N_\phi - 1$ is itself tridiagonal and of order $(N_\theta - 1)$. The off-diagonal submatrices C_j, $j = 1, 2, \ldots, N_\phi - 2$ are likewise square and of order $(N_\theta - 1)$ but diagonal in form. These characteristics follow from the fact that equation (22), which determines the form of A, is a five-point symmetric difference approximation. The non-zero entries of the submatrix A_j consist of the coupling coefficients of a grid point with its immediate grid neighboring points on the same horizontal line, while the submatrix C_j consists of diagonal entries representing the coupling coefficients of a grid point with its immediate grid neighboring points on the horizontal lines vertically above and below.

The matrix E in equation (29) is square, of the same order as A, and diagonal with positive entries, by virtue of equation (24c). Finally, note that the entries of A and E depend only on the j-index and are independent of i.

Now, define a square matrix V of order $(N_\theta - 1)(N_\phi - 1)$ by $V = E^{1/2}U$, where $E^{1/2}$ is the diagonal matrix consisting of entries which are equal, respectively, to the square roots of the elements of E. With this definition, equation (29) may be transformed to

$$\tilde{A}V = E^{-1/2}AE^{-1/2}V = \lambda V, \tag{31}$$

through pre-multiplication by the diagonal matrix $E^{-1/2}$, the inverse of $E^{1/2}$ formed by taking reciprocals of the respective diagonal entries of $E^{1/2}$. The matrix $\tilde{A} \equiv E^{-1/2} A E^{-1/2}$, transformed from A by the pre- and post-multiplication of a diagonal matrix, retains the symmetry property of A.

In order to determine the fundamental (or smallest) eigenvalue of the matrix $\tilde{A}$, an iterative procedure known as the power method (Reference 5, pp. 147 ff; Reference 6, pp. 355-356) will be utilized. As applied to problem (31), the algorithm for the power method involves the sequence of vectors defined by

$$V^{(m+1)} = \lambda^{(m)}\tilde{A}^{-1}V^{(m)}, \qquad m = 1, 2, \ldots, \tag{32}$$

where the sequence of scalars $\lambda^{(m)}$ is given by

$$\lambda^{(m)} = \frac{(V^{(m)}, V^{(m)})}{(\tilde{A}^{-1}V^{(m)}, V^{(m)})}, \qquad m = 1, 2, \ldots. \tag{33}$$

The limit of the vectors $V^{(m)}$ as $m \to \infty$ is the eigenvector associated with the fundamental eigenvalue of $\tilde{A}$. The fundamental eigenvalue, in turn, is approximated by the finite Rayleigh quotient (33), which involves a ratio of inner products. In terms of the original vector U of equation (29), it is seen that $U^{(m)} = E^{-1/2} V^{(m)}$ and $\tilde{A}^{-1} = E^{1/2} A^{-1} E^{1/2}$, so that equation (32) becomes

$$U^{(m+1)} = \lambda^{(m)}A^{-1}EU^{(m)}, \qquad m = 1, 2, \ldots. \tag{34}$$

Furthermore, the Rayleigh quotient (33) in terms of the original vector U is equivalent to

$$\lambda^{(m)} = \frac{(U^{(m)}, EU^{(m)})}{(A^{-1}EU^{(m)}, EU^{(m)})}, \qquad m = 1, 2, \ldots. \tag{35}$$

As an initial estimate for the iterations (34), $U^{(1)}$ is defined so that components associated with grid points interior to the spherical triangle T (a subset of the

rectangular interior grid points enumerated by the subscripts $i = 1, 2, 3, \ldots, N_\theta - 1$; $j = 1, 2, 3, \ldots, N_\phi - 1$) are assigned the value unity and components associated with grid points coincident with the spherical triangle boundary or exterior to T are assigned zero values. That is, $U^{(1)}_{i,j} = 0$ for those rectangular interior grid points satisfying relation (26), and $U^{(1)}_{i,j} = 1$ for those rectangular interior grid points which satisfy the reverse inequality:

$$\cot \phi_j > a \cos \theta_i + b \sin \theta_i .$$

In order to implement the power method as expressed by equations (34) and (35), it is necessary to solve equations of the general form $AU = F$ for the vector U, where F represents the vector iterates $EU^{(m)}$. For this purpose, the iterative method of point successive overrelaxation is applied to the system of linear equations (22). This method (Reference 4, pp. 58-59, for example) produces iterates $U^{(k)}$ whose components are given by

$$U^{(k+1)}_{i,j} = \frac{\omega}{a_j} \left[b_j U^{(k)}_{i+1,j} + c_j U^{(k)}_{i,j+1} + b_j U^{(k+1)}_{i-1,j} + c_{j-1} U^{(k+1)}_{i,j-1} + F_{i,j} \right] + (1 - \omega) U^{(k)}_{i,j}, \quad k = 1, 2, \ldots . \tag{36}$$

In equation (36), ω is the scalar relaxation factor (evaluated by a method to be described), and the superscripts k and (k+1) indicate an iteration process distinct from the m-iterates specified in the power method described above. In fact, the vectors U and F that appear in equation (36) depend upon the iteration index m, although this has not been indicated explicitly, in order to preserve legibility. Note that, according to equations (23d) and (24), $a_j \neq 0$, so that singularity problems do not arise. The k-iterations arising from use of equation (36) will be called the inner iterations, so as to distinguish them from the m-iterations arising from use of equations (34) and (35), which will be called the outer iterations. The vectors F are defined by $F^{(m)} = EU^{(m)}$ and are k-independent

(i.e., constant for the inner iterations). Since $E = \text{diag}\,(e_j)$, the following component relationship holds:

$$F_{i,j} = e_j U_{i,j}, \quad \text{for } i = 1, 2, \ldots, N_\theta - 1; \quad j = 1, 2, \ldots, N_\phi - 1. \tag{37}$$

The range of indexing for the i, j subscripts shown in equation (37) also applies to the inner iterations (36). During the inner iterations, the convergence parameters,

$$\epsilon^{(k)} \equiv \max_{\substack{1 \le i \le N_\theta - 1 \\ 1 \le j \le N_\phi - 1}} \left| U_{i,j}^{(k+1)} - U_{i,j}^{(k)} \right|, \quad k = 1, 2, \ldots \tag{38a}$$

and

$$r^{(k)} \equiv \epsilon^{(k)} / \epsilon^{(k-1)}, \quad k = 2, 3, \ldots, \tag{38b}$$

are calculated for use in the evaluation of the relaxation factor ω. Before discussing this evaluation procedure, it is worthwhile to note that the theoretical demonstration of convergence of the successive overrelaxation iterates (36) for any initial vector $U^{(1)}$ chosen follows from the Ostrowski-Reich theorem (Reference 7, p. 123) for a relaxation factor in the range $0 < \omega < 2$. This theorem depends upon the positive definite property of the matrix A, which in turn follows (Reference 4, p. 23) from the fact that A may be shown to be a symmetric irreducibly diagonally dominant matrix with positive diagonal entries, by virtue of equation (23d) and certain graph theoretic arguments (Reference 4, p. 20).

Although the method of successive overrelaxation will converge for all relaxation factors ω such that $0 < \omega < 2$, the most rapid convergence occurs for an optimal value denoted ω_{opt}, where $1 < \omega_{opt} < 2$. A theoretical expression for ω_{opt} exists (Reference 4, p. 110) since the Jacobi matrix associated with the matrix A is cyclic of index 2. This expression depends on the spectral

radius of the associated Jacobi matrix, a quantity that is not, unfortunately, known a priori. In order to overcome this difficulty in determining ω_{opt}, described (Reference 6, p. 257) as "perhaps the most important problem" in the practical use of successive overrelaxation, a numerical technique (Reference 6, pp. 369-370) utilizing the point Gauss-Seidel iterative method is applied. If ω is set equal to unity in equation (36), then the second term on the right side of the equation vanishes and the successive overrelaxation method reduces to the point Gauss-Seidel method. In this case, the ratio of maximum component norms for successive inner iterates of the vector U defined in equations (38) will converge to a value,

$$\lim_{k \to \infty} r^{(k)} = r \leq 1, \tag{39}$$

equal to the square of the desired spectral radius of the associated Jacobi matrix mentioned above. Then ω_{opt} can be computed by the formula

$$\omega_{opt} = \frac{2}{1 + \sqrt{1 - r}}. \tag{40}$$

A method for defining a vector relaxation factor $\omega = \omega_j$, dependent upon the grid spacing parameters N_ϕ and ϕ_j in the ϕ-direction and not requiring Gauss-Seidel iterations, for use in the successive overrelaxation method (36) was also attempted, but without convergence success.

In the implementation of the numerical technique described above, four additional convergence parameters are selected initially before the finite difference approximation is applied. Two of these parameters, ϵ_{INNER} and ϵ_{OUTER}, are specified small positive numbers such that

$$0 < \epsilon_{INNER}, \quad \epsilon_{OUTER} << 1, \tag{41}$$

and which are used as criteria for evaluating the convergence of the inner and outer iteration schemes, respectively. Two other parameters, k_{max} and m_{max},

are specified positive integers, the first of which is used to effect the convergence of r in equation (39) and also as an upper bound on the number of inner iterations permitted and the second of which is used simply as an upper bound on the number of outer iterations permitted. These four pre-selected parameters are utilized in the numerical implementation as follows, in a modification of a method suggested (Reference 6, pp. 375-376) for the solution of the finite eigenvalue problem on a digital computer. First, the point Gauss-Seidel iterative method (36), in which $\omega = 1$, is applied using the initial vector estimate $U^{(1)}$, as previously described. After each such inner iteration is completed, the norm $\epsilon^{(k)}$ is computed by equation (38a). If for some value of k in the range $1 \leq k \leq k_{max}$ (say $k = K$), it is found that $\epsilon^{(K)} < \epsilon_{INNER}$, then the inner iterations are regarded as having converged and r is taken to be the value $r^{(K)}$ and ω_{opt} is computed by formula (40). Henceforth, all subsequent inner iterations use the point successive overrelaxation method (36), in which $\omega = \omega_{opt}(r^{(K)})$, and an initial vector estimate is computed as described below. If, however, $\epsilon^{(k)} \geq \epsilon_{INNER}$ for all $k = 1, 2, \ldots, k_{max}$, then the inner iterations do not converge and r is set equal to $r^{(k_{max})}$ and ω_{opt} is computed using this value for r. Henceforth, all subsequent inner iterations use successive overrelaxation in which $\omega = \omega_{opt}(r^{(k_{max})})$. In the latter instance, the non-convergence of the inner iterations is disregarded during the first ($m = 1$) outer iteration. However, if, in any subsequent ($m = 2, 3, \ldots$) outer iteration, the inner iterations fail to converge (i.e., $\epsilon^{(k)} \geq \epsilon_{INNER}$ for all $k = 1, 2, \ldots, k_{max}$), then the eigenvalue problem is regarded as non-convergent. In such case of problem non-convergence, the problem may be attempted again by properly adjusting the pre-selected convergence parameters, e.g., by increasing the value of k_{max} or that of ϵ_{INNER} or both.

When convergence of the inner iterations is achieved (or, alternatively, after k_{max} inner iterations during the first outer iteration), then the Rayleigh quotient

(35) may be used to approximate the fundamental eigenvalue $\lambda^{(m)}$ for the m^{th} outer iteration. The vector inner products on the right side of equation (35) may be written in component form as $\lambda^{(m)} = P/Q$, where

$$P = (U^{(m)},\ EU^{(m)}) = \sum_{i=1}^{N_\theta - 1} \left(\sum_{j=1}^{N_\phi - 1} \frac{F_{i,j}^2}{e_j} \right) \tag{42a}$$

and

$$Q = (A^{-1}EU^{(m)},\ EU^{(m)}) = \sum_{i=1}^{N_\theta - 1} \left(\sum_{j=1}^{N_\phi - 1} F_{i,j} U_{i,j} \right). \tag{42b}$$

In the double summation expression (42a), the vector EU is given by the components $F_{i,j}$, while the vector U (prior to initiation of the most recent set of inner iterations) must be retrieved by the ratio $F_{i,j}/e_j$ of components. In the double summation expression (42b), the vector $A^{-1}EU$ (following completion of the most recent set of inner iterations) is given by the components $U_{i,j}$ upon convergence of the inner iterations. Now, for the second and all subsequent outer iterations, convergence of the outer iterations and of the approximation to the fundamental eigenvalue occurs when

$$|\lambda^{(m)} - \lambda^{(m-1)}| < \epsilon_{OUTER}, \quad 2 \le m \le m_{max}. \tag{43}$$

In this event, $\lambda^{(m)}$ is the calculated fundamental eigenvalue which approximately satisfies the eigenvalue problem (11). If, however,

$$|\lambda^{(m)} - \lambda^{(m-1)}| \ge \epsilon_{OUTER} \tag{44}$$

for all $m = 2, 3, \ldots, m_{max}$, then the fundamental eigenvalue does not converge within the allotted number m_{max} of outer iterations. This situation may be alleviated by properly adjusting the pre-selected convergence parameters, e.g., by increasing the value of m_{max} or that of ϵ_{OUTER} or both. Finally, if inequality (44) is satisfied for some outer iteration m, where $2 \le m < m_{max}$, then the outer iteration procedure has not converged, but the vector U is re-initialized for the

inner iterations utilizing point successive overrelaxation (36) by the power method (34), which may be written in component form as

$$U_{i,j}^{(m+1)} = \lambda^{(m)} U_{i,j}^{(m)}, \quad \text{for } i = 1, 2, \ldots, N_\theta - 1; \; j = 1, 2, \ldots, N_\phi - 1. \tag{45}$$

In equation (45), the vector components on the right side are those that result following completion of the inner iterations for outer iteration m. The vector components on the left are those to be utilized as the initial vector estimate for the first (k = 1) inner iteration of outer iteration number (m + 1) as well as the components to be used in re-evaluating the vector F by equation (37).

This completes the discussion of the iterative method of solution of the finite difference equations by point successive overrelaxation and the subsequent iterative determination of the fundamental eigenvalue by the power method utilizing the Rayleigh quotient. Application of these techniques is clarified by the algorithmic presentation within Appendix A of the methods discussed in Sections II and III.

SECTION IV

ANALYTIC SOLUTIONS FOR SPECIAL CASES

In this section, the elliptic partial differential equation (12) will be solved analytically, or exactly, for certain special cases, although, as has been remarked previously, an analytic solution is not known for the general case. The exact solutions to be found will be useful in providing checks upon numerical calculations based upon the finite difference approximation.

In order to solve equation (12) analytically, the separation of variables technique will be employed (Reference 2, pp. 510-512), in which

$$u(\theta, \phi) = X(\theta)\, Y(\phi). \tag{46}$$

Substitution of the separated form (46) into equation (12) yields, after re-arrangement,

$$-\frac{1}{X(\theta)}\frac{d^2X(\theta)}{d\theta^2} = \frac{\sin\phi}{Y(\phi)}\left(\frac{d^2Y(\phi)}{d\phi^2}\sin\phi + \frac{dY(\phi)}{d\phi}\cos\phi\right) + \lambda \sin^2\phi. \tag{47}$$

Since the left side of equation (47) is a function of θ only, and the right side of the equation is a function of ϕ only, both sides may be set equal to a separation parameter k^2, a constant independent of both θ and ϕ. In this case, the equation for θ,

$$\frac{d^2X(\theta)}{d\theta^2} + k^2X(\theta) = 0,$$

is readily seen to have the solution

$$X(\theta) = A \sin k\theta + B \cos k\theta, \tag{48}$$

where A and B are constants. The boundary condition (11b) requires that $u(0,\phi) = u(\Theta, \phi) = 0$, so that the solution (48) becomes

$$X(\theta) = A \sin\left(\frac{\pi}{\Theta}\right)\theta, \tag{49}$$

where $k = \pi/\Theta$ is chosen so that $X(\theta)$ vanishes only at the endpoints of the interval $0 \le \theta \le \Theta$. The equation for ϕ, from equation (47),

$$\sin^2\phi \frac{d^2Y(\phi)}{d\phi^2} + \sin\phi\cos\phi \frac{dY(\phi)}{d\phi} + (\lambda \sin^2\phi - k^2)\, Y(\phi) = 0,$$

may be transformed by the substitutions $\cos\phi = z$, $Y(\cos\phi) = v(z)$ to the following form:

$$(1 - z^2)^2 \frac{d^2v(z)}{dz^2} - 2z(1 - z^2) \frac{dv(z)}{dz} + [\lambda(1 - z^2) - k^2]\, v(z) = 0. \qquad (50)$$

The solutions to equation (50) are known (Reference 2, pp. 327, 511) to be the associated Legendre functions of order k,

$$v(z) = P_{n,k}(z) = (1 - z^2)^{k/2} \frac{d^k}{dz^k} P_n(z), \quad k = 0, 1, 2, \ldots, n, \qquad (51)$$

where n is defined by $\lambda = n(n+1)$. The Legendre functions of order zero, $P_n(z) = P_{n,0}(z)$, are polynomials in z of degree n.

Consider the special case $k = n$. For this choice, the derivative factor in equation (51) reduces to a constant and v(z) becomes a multiple of $(\sin\phi)^k$. In this case, the solution (46) is

$$u(\theta, \phi) = A \sin\left(\frac{\pi\theta}{\Theta}\right) (\sin\phi)^{\pi/\Theta}, \qquad (52)$$

where A is an arbitrary constant, and the corresponding eigenvalue is

$$\lambda = \frac{\pi}{\Theta}\left(\frac{\pi}{\Theta} + 1\right).$$

Note that for $A \neq 0$, the eigenfunction (52) vanishes only for $\theta = 0, \Theta$ and $\phi = 0, \pi$ in the domain $0 \le \theta \le \Theta < 2\pi$; $0 \le \phi \le \pi$. Thus, equation (52) represents a solution for the case in which the spherical triangle has degenerated to a two-sided spherical wedge-shaped domain bounded by meridional arcs extending from the north to the south pole. In fact, it may be readily demonstrated that the

eigenfunction (52) satisfies equation (12) by direct substitution, and, as noted, it further satisfies the boundary conditions (11b). Hence, the eigenfunction (52) is an exact analytic solution to problem (11), where

$$\lambda = \frac{\pi}{\Theta}\left(\frac{\pi}{\Theta} + 1\right)$$

for any Θ in the range $0 < \Theta < 2\pi$. The original restriction of the solution (51) that $k = n = \pi/\Theta$ be a positive integer may thus be removed in this special case. In terms of the constant parameters a,b of inequality (9), the wedge-shaped domain is specified by the limits $a = 0, b \to -\infty$ when $\Theta \leq \pi$; however, when $\Theta > \pi$, the wedge does not appear as a limiting case of the spherical triangle.

Now consider the special case $k = n - 1$. For this choice, the derivative factor in the associated Legendre function (51) reduces to a term linear in z. This term linear in z is, in fact, merely a constant multiple of z, since the Legendre functions $P_n(z)$ are polynomials in z containing terms only of even or odd powers of z, depending as n is even or odd, respectively. It is seen then that v(z) is a multiple of $(\sin\phi)^k \cos\phi$ in this case, and the solution (46) is

$$u(\theta, \phi) = A \sin\left(\frac{\pi\theta}{\Theta}\right)(\sin\phi)^{\pi/\Theta}\cos\phi, \tag{53}$$

where A is an arbitrary constant, and the corresponding eigenvalue is

$$\lambda = n(n+1) = (k+1)(k+2) = \left(\frac{\pi}{\Theta} + 1\right)\left(\frac{\pi}{\Theta} + 2\right)$$

For $A \neq 0$, the eigenfunction (53) has the same zeroes as that of the previous eigenfunction (52), viz., $\theta = 0$, Θ and $\phi = 0, \pi$, and, in addition, it vanishes for $\phi = \pi/2$. Thus, equation (53) represents a solution for the spherical triangle defined by the domain $0 \leq \theta \leq \Theta < 2\pi$; $0 \leq \phi \leq \pi/2$. Equivalently stated, this

triangle is bounded by two meridional arcs and the equator, specified by setting $a = b = 0$ in inequality (9). In this special case also, the eigenfunction (53) may be shown to satisfy the elliptic partial differential equation (12) by direct substitution. The boundary conditions (11b) are fulfilled for the particular spherical triangle described above. Hence, the eigenfunction (53) is an exact analytic solution to problem (11), where

$$\lambda = \left(\frac{\pi}{\Theta} + 1\right)\left(\frac{\pi}{\Theta} + 2\right)$$

for any Θ in the interval $0 < \Theta < 2\pi$. The original restriction of the solution (51) that $k = n - 1 = \pi/\Theta$ be a positive integer may be removed in this special case as well.

Consideration of further special cases obtained when $k = n - 2, n - 3, \ldots$ does not lead to spherical triangles which can be readily identified, so this course will not be pursued. However, it is of interest to consider the two special cases described above in the event that $\Theta = 2\pi$, a possibility that was specifically excluded in previous discussion. With $\Theta = 2\pi$, the solution (52) becomes

$$u(\theta, \phi) = A \sin\frac{\theta}{2} (\sin\phi)^{1/2},$$

and the corresponding eigenvalue is $\lambda = 3/4$. Also, the two-sided spherical wedge-shaped domain now becomes the entire surface of the sphere except for a boundary great circle arc extending between the north and south poles. This particular domain may be viewed equivalently as the exterior of a spherical triangle in the limit when $\Theta = 0$. Such an equivalent view will be of significance in the discussion of Section VI. In the second special case, the solution (53) becomes $u(\theta, \phi) = A \sin(\theta/2)(\sin\phi)^{1/2} \cos\phi$, and the corresponding eigenvalue is $\lambda = 15/4$. In this instance, the spherical triangle domain degenerates to the entire upper hemisphere except for a boundary great circle arc extending from the north pole to the equator, and the domain is defined by the values $a = b = 0$, $\Theta = 2\pi$.

SECTION V

DISCUSSION OF NUMERICAL RESULTS

The iterative solution of the finite difference equations by successive over-relaxation has been adapted to an electronic digital computer program for calculating the fundamental eigenvalue of a spherical triangle. The mathematical and theoretical basis for the solution has been discussed previously in Sections II and III, and the algorithm for the calculation is presented in Appendix A. In the present section, numerical results for a number of cases of interest are presented and discussed.

The first series of spherical triangles to be considered consists of triangles containing two right angles where the boundary great circle arcs are formed by the equator $z = 0$ and two meridional arcs. In terms of the spherical triangle parameters, such a triangle is specified by $a = 0$, $b = 0$ and Θ, where $0 < \Theta < 2\pi$. It will be recognized that this particular case was solved analytically in Section IV for the fundamental eigenvalue

$$\lambda = \left(\frac{\pi}{\Theta} + 1\right)\left(\frac{\pi}{\Theta} + 2\right).$$

Table 1 displays calculated values for the fundamental eigenvalue λ for each of three values for the spherical triangle parameter Θ and for various rectangular grid parameters, N_θ and N_ϕ. All the grids utilized a grid spacing parameter $\gamma = 1$, i.e., the grid spacing in both the θ- and ϕ-directions was constant, as specified in equations (13) and (14). The criteria adopted for iterative convergence for use in this table and in all other numerical results discussed herein are $\epsilon_{INNER} = \epsilon_{OUTER} = 10^{-6}$. For comparative purposes, the exact value for the fundamental eigenvalue, as determined from the analytic relationship $\lambda = \lambda(\Theta)$ is also shown in Table 1. Other columns in Table 1 include the calculated value for the optimal scalar relaxation factor ω, the required number m of outer iterations

Table 1
Fundamental Eigenvalues of Double Right Spherical Triangles (a=b=0)
Using Constant Grid Spacing in the ϕ-Direction (γ=1)

Spherical Triangle Parameter Θ	Rectangular Grid Parameters		Fundamental Eigenvalue λ		Optimal Scalar Relaxation Factor ω	Required Number of Outer Iterations m	Required Number of Gauss-Seidel Inner Iterations k_1	Required Number of S.O.R. Inner Iterations at Convergence k_m
	N_θ	N_ϕ	Calculated Value	Exact Value				
π	10	10	5.831	6	1.460	8	85	24
π	20	20	5.958	6	1.695	8	100	48
π	30	30	5.981	6	1.796	8	100	71
π	40	40	5.990	6	1.860	8	100	99
$\pi/2$	10	10	11.628	12	1.506	8	100	27
$\pi/2$	20	20	11.907	12	1.723	10	100	49
$\pi/2$	30	30	11.959	12	1.807	11	100	73
$\pi/2$	40	40	11.977	12	1.850	11	150	97
$\pi/3$	10	10	19.338	20	1.518	12	100	27
$\pi/3$	20	20	19.836	20	1.729	13	100	50
$\pi/3$	30	30	19.927	20	1.806	13	100	78
$\pi/3$	40	40	19.959	20	1.846	13	150	110

to achieve convergence in λ, the required number $k_1 = K$ of inner iterations to achieve convergence of U by the Gauss-Seidel method for the first outer iteration, and the required number k_m of inner iterations to achieve convergence of U by successive overrelaxation (S.O.R.) for the final outer iteration. The upper limits on the number of iterations permitted for inner and outer convergence were initially selected to be $k_{max} = 100$ and $m_{max} = 50$, respectively. This value for m_{max} was always found to be more than sufficient to promote outer convergence. However, the value of $k_{max} = 100$ was not always sufficient to permit inner convergence by successive overrelaxation. (It will be recalled from the discussion in Section III that non-convergence of the Gauss-Seidel iterations during the first outer iteration is disregarded.) In such cases of insufficiency, the value of k_{max} was incremented by 50 successively until inner convergence resulted. The number of increments $\Delta k_{max} = 50$ necessary to promote inner convergence can be ascertained by examination of the column of values for k_1. In Table 1, it is seen that $k_{max} = 100$ was sufficient for inner convergence except for the two $N_\theta = N_\phi = 40$ grids when $\Theta = \pi/2$ and $\Theta = \pi/3$, in which cases the increase to $k_{max} = 150$ was then sufficient to promote inner convergence. Further examination of this same column of values reveals that only in one instance (for the $N_\theta = N_\phi = 10$ grid when $\Theta = \pi$) did the Gauss-Seidel iterations converge for $k_1 < k_{max}$. In all other cases, $k_1 = k_{max}$, indicating non-convergence of the Gauss-Seidel iterations during the first outer iteration. (An alternate, but less likely, possibility is that the Gauss-Seidel iterations converged on precisely the final permitted iteration, number k_{max}.)

The significant results provided by Table 1 include the qualitative fact that as the rectangular grid becomes finer (as measured by an increase in the parameters N_θ and N_ϕ), the calculated value for the fundamental eigenvalue λ becomes more accurate. Quantitatively speaking, the relative error in λ, given by

$(\lambda_{exact} - \lambda_{calculated})/\lambda_{exact}$, is approximately 0.03 for the $N_\theta = N_\phi = 10$ grids, 0.008 for the $N_\theta = N_\phi = 20$ grids, 0.003 for the $N_\theta = N_\phi = 30$ grids, and 0.002 for the $N_\theta = N_\phi = 40$ grids. These relative errors apply approximately for the three values of the spherical triangle parameter Θ, but the relative errors, for a given set of grid parameters, are smallest for the case $\Theta = \pi$ and largest for the case $\Theta = \pi/3$. Of course, use of a finer grid results in a more accurate eigenvalue but also entails a substantially greater number of calculations to complete the successive overrelaxation method. Note also that the convergence to the exact value of λ with increasing grid parameters occurs monotonically for each of the three Θ values. A similar phenomenon occurs in the calculated values for the optimal scalar relaxation factor ω, viz., the values of ω increase with the increasing grid parameters. Finally, this same phenomenon is repeated in the required number of inner and outer iterations. However, the increase in required outer iterations m with increasing grid parameters is negligible, while the increase in required inner iterations k_m just prior to convergence is considerable. Note also that the required number k_m of inner iterations for the final outer iteration is generally substantially fewer than the required number k_1 of inner iterations for the first outer iteration. This last characteristic may be ascribed to the fact that the convergence criteria are invariant (equal to the values $\epsilon_{INNER} = \epsilon_{OUTER} = 10^{-6}$) throughout the iterative process. Most of the other phenomena delineated above are due to the fact that convergence occurs more slowly for a finer grid than for a coarse grid.

The next series of results, as displayed in Table 2, is intended to investigate the effect of adopting a variable grid spacing in the ϕ-direction, as discussed previously in Section II. For this purpose, a value for the grid spacing parameter of $\gamma = 2$ was chosen. This produces a grid in which the density of grid points increases toward the poles (recall that a singularity occurs at the north pole, $\phi = 0$)

Table 2
Fundamental Eigenvalues of Double Right Spherical Triangles (a=b=0)
Using Variable Grid Spacing in the ϕ-Direction ($\gamma = 2$)

Spherical Triangle Parameter Θ	Rectangular Grid Parameters		Fundamental Eigenvalue λ		Optimal Scalar Relaxation Factor ω	Required Number of Outer Iterations m	Required Number of Gauss-Seidel Inner Iterations k_1	Required Number of S.O.R. Inner Iterations at Convergence k_m
	N_θ	N_ϕ	Calculated Value	Exact Value				
π	10	10	5.750	6	1.494	8	100	25
π	20	20	5.931	6	1.716	8	100	49
π	30	30	5.969	6	1.807	9	100	73
π	40	40	5.983	6	1.852	9	150	97
$\pi/2$	10	10	11.368	12	1.519	10	100	26
$\pi/2$	20	20	11.798	12	1.730	11	100	49
$\pi/2$	30	30	11.910	12	1.811	11	100	73
$\pi/2$	40	40	11.949	12	1.847	11	150	104
$\pi/3$	10	10	19.123	20	1.523	11	100	26
$\pi/3$	20	20	19.609	20	1.731	14	100	49
$\pi/3$	30	30	19.825	20	1.801	13	100	81
$\pi/3$	40	40	19.902	20	1.847	13	150	105

and decreases toward the equator, in a fashion symmetrically arranged about the equator. The same spherical triangles and the same values for the rectangular grid parameters are considered as in Table 1. The outcome of using this particular variable grid spacing on the calculated values of λ is seen to be larger relative errors in each of the 12 cases considered, as compared to the results of Table 1 for a constant grid spacing. Hence, this method of varying the grid spacing in the ϕ-direction in order to account for the singularity in ϕ does not achieve the desired effect. Virtually all other qualitative characteristics noted in the Table 1 results also apply to Table 2, however. In particular, more refined grids produce more accurate calculated values for the fundamental eigenvalue, and the convergence to the known exact value for λ occurs monotonically in each of the three Θ cases.

A variable grid spacing in the ϕ-direction based upon the parametric value $\gamma = 1/2$ was next investigated, and the results are displayed in Table 3. This value of γ produces a grid in which the density of grid points increases toward the equator and decreases toward the poles, again in a manner symmetrical with respect to the equator. The same spherical triangles with two right angles and the same values for the rectangular grid parameters are considered as in Tables 1 and 2. This particular variable grid spacing produces calculated values of λ with larger relative errors than both Tables 1 and 2 for the $\Theta = \pi$ cases and for the $\Theta = \pi/2$ cases for the coarser $N_\theta = N_\phi = 10$ and $N_\theta = N_\phi = 20$ grids. However, for the finer $N_\theta = N_\phi = 30$ and $N_\theta = N_\phi = 40$ grids when $\Theta = \pi/2$, the calculated λ are more accurate in the $\gamma = 1/2$ grid spacing (Table 3) than in the $\gamma = 2$ grid spacing (Table 2), though not so accurate as in the constant grid spacing (Table 1). For the case $\Theta = \pi/3$, the result for λ in Table 3 is least accurate for the coarsest $N_\theta = N_\phi = 10$ grid, but most accurate for the finer three grids, even when compared against the constant grid spacing results. For $\Theta = \pi/3$,

Table 3
Fundamental Eigenvalues of Double Right Spherical Triangles (a=b=0)
Using Variable Grid Spacing in the ϕ-Direction ($\gamma = 1/2$)

Spherical Triangle Parameter Θ	Rectangular Grid Parameters		Fundamental Eigenvalue λ		Optimal Scalar Relaxation Factor ω	Required Number of Outer Iterations m	Required Number of Gauss-Seidel Inner Iterations k_1	Required Number of S.O.R. Inner Iterations at Convergence k_m
	N_θ	N_ϕ	Calculated Value	Exact Value				
π	10	10	5.118	6	1.427	8	73	22
π	20	20	5.592	6	1.673	8	100	45
π	30	30	5.773	6	1.780	8	100	62
π	40	40	5.856	6	1.844	8	100	85
$\pi/2$	10	10	10.692	12	1.488	10	98	26
$\pi/2$	20	20	11.739	12	1.713	11	100	46
$\pi/2$	30	30	11.919	12	1.797	11	100	75
$\pi/2$	40	40	11.969	12	1.850	11	100	94
$\pi/3$	10	10	19.061	20	1.508	11	100	27
$\pi/3$	20	20	19.888	20	1.720	13	100	52
$\pi/3$	30	30	19.961	20	1.806	13	100	74
$\pi/3$	40	40	19.979	20	1.848	13	150	104

the relative error in λ is approximately 0.047 for the $N_\theta = N_\phi = 10$ grid, 0.006 for the $N_\theta = N_\phi = 20$ grid, 0.002 for the $N_\theta = N_\phi = 30$ grid, and 0.001 for the $N_\theta = N_\phi = 40$ grid. These relative errors in λ are considerably smaller than those for the corresponding grids in the cases $\Theta = \pi/2$ and $\Theta = \pi$. The conclusion appears to be that variable grid spacing of the type used in the Table 3 results can produce a more accurate calculated value for the fundamental eigenvalue than that produced by use of constant grid spacing, but the relative accuracies depend upon the characteristics of the spherical triangle under consideration. Other convergence qualities noted in the previous Tables 1 and 2 results for the remaining parameters displayed also hold for the Table 3 results.

The abbreviated display in Table 4 considers the special case $\Theta = 2\pi$ only, in which the spherical triangle degenerates to the upper hemisphere with boundaries consisting of the equator and one meridional great circle arc (a "slit") extending from the north pole to the equator. This degeneracy was specifically considered at the end of Section IV, and the analytic relationship

$$\lambda = \left(\frac{\pi}{\Theta} + 1\right)\left(\frac{\pi}{\Theta} + 2\right)$$

yields an exact value for the fundamental eigenvalue of 15/4. The same sequence of values for the rectangular grid parameters is adopted in Table 4 as in the earlier tables, and constant grid spacing in the ϕ-direction with $\gamma = 1$ is utilized, as was the case for Table 1. Once again, the finer grids are seen to produce more accurate calculated values of λ with convergence to the known exact value occurring monotonically, but in this instance the convergence is monotone decreasing. In the previous results of Tables 1, 2, and 3, the convergence was always monotonic and increasing. Otherwise, the results of Table 4 show the usual convergence properties noted earlier and serve primarily to verify the analytic solution for a particular special case.

Table 4
Fundamental Eigenvalue of Slit Upper Hemisphere (a=b=0; $\Theta = 2\pi$)
Using Constant Grid Spacing in the ϕ-Direction ($\gamma = 1$)

Spherical Triangle Parameter Θ	Rectangular Grid Parameters		Fundamental Eigenvalue λ		Optimal Scalar Relaxation Factor ω	Required Number of Outer Iterations m	Required Number of Gauss-Seidel Inner Iterations k_1	Required Number of S.O.R. Inner Iterations at Convergence k_m
	N_θ	N_ϕ	Calculated Value	Exact Value				
2π	10	10	3.845	3.75	1.385	10	59	21
2π	20	20	3.826	3.75	1.647	10	100	42
2π	30	30	3.806	3.75	1.760	10	100	59
2π	40	40	3.794	3.75	1.837	9	100	83

The next series of results in Table 5 investigates another of the special cases discussed previously in Section IV, that of the spherical wedge. It will be recalled that the spherical wedge is a degenerate case of the spherical triangle which is bounded by two meridional great circle arcs extending from pole to pole, and it is specified by the limits $a = 0$, $b \to -\infty$ when $\Theta \leq \pi$. The exact value for the fundamental eigenvalue is given by

$$\lambda = \frac{\pi}{\Theta}\left(\frac{\pi}{\Theta} + 1\right).$$

When $\Theta = \pi$ with $a = 0, b \to -\infty$, the spherical wedge becomes a hemisphere, with fundamental eigenvalue $\lambda = 2$. However, when Θ assumes a value in the range $\pi < \Theta \leq 2\pi$ with $a = 0$, $b \to -\infty$, the domain specified is still the hemispherical wedge, with the corresponding eigenvalue $\lambda = 2$. As can be seen from inequality (9), the only value of ϕ in the domain for $a = 0$, $b \to -\infty$, and θ in the range $\pi < \theta < 2\pi$ is $\phi = 0$, the north pole. For numerical purposes, the value adopted for b in the Table 5 results was -10^9. The standard sequence of values for the rectangular grid parameters is adopted as in the earlier tables, and constant grid spacing is utilized. For both the quarter-spherical wedge ($\Theta = \pi/2$) and the hemispherical wedge ($\Theta = \pi$), the convergence to the known exact value of λ is monotonically increasing, as in the first three tables, with the more refined grids. Also, the calculated values for the fundamental eigenvalue are seen to possess considerable accuracy for all grids. Now in the cases $\Theta = 3\pi/2$ and $\Theta = 2\pi$, the convergence in λ is also monotonically increasing with the refinement in the grids, but the corresponding relative errors are larger than for the smaller values of Θ. This is undoubtedly due to the fact that a larger proportion of the grid points in the $\Theta = 3\pi/2, 2\pi$ cases are "superfluous," i.e., proportionately fewer grid points occur interior to the spherical wedge domain than in the corresponding cases for $\Theta = \pi/2$ and $\Theta = \pi$, for a given set of rectangular

Table 5
Fundamental Eigenvalues of Spherical Wedges (a=0, b→- ∞)
Using Constant Grid Spacing in the ϕ-Direction ($\gamma = 1$)

Spherical Triangle Parameter Θ	Rectangular Grid Parameters		Fundamental Eigenvalue λ		Optimal Scalar Relaxation Factor ω	Required Number of Outer Iterations m	Required Number of Gauss-Seidel Inner Iterations k_1	Required Number of S.O.R. Inner Iterations at Convergence k_m
	N_θ	N_ϕ	Calculated Value	Exact Value				
$\pi/2$	10	10	5.926	6	1.543	8	100	29
$\pi/2$	20	20	5.982	6	1.750	8	100	54
$\pi/2$	30	30	5.992	6	1.808	9	100	95
$\pi/2$	40	40	5.995	6	1.854	9	150	122
π	10	10	1.977	2	1.572	6	100	31
π	20	20	1.994	2	1.774	6	100	59
π	30	30	1.997	2	1.824	6	150	101
π	40	40	1.999	2	1.838	6	200	177
$3\pi/2$	10	10	1.828	2	1.512	6	100	26
$3\pi/2$	20	20	1.852	2	1.722	6	100	48
$3\pi/2$	30	30	1.917	2	1.830	6	100	73
$3\pi/2$	40	40	1.961	2	1.848	6	150	90
2π	10	10	1.929	2	1.465	6	83	23
2π	20	20	1.972	2	1.686	6	100	45
2π	30	30	1.982	2	1.788	6	100	62
2π	40	40	1.987	2	1.845	6	150	83

grid parameters. Nonetheless, convergence to the proper exact value of λ does occur monotonically for all Θ values in Table 5. Convergence properties of other parameters displayed in the table are similar to those observed in previous results.

This concludes the discussion of numerical results obtained for all the special cases considered in Section IV for which analytical solutions were obtained, thereby providing known exact values for the fundamental eigenvalues. A final series of results is presented in Table 6 for an archetypical case (a so-called oblique spherical triangle) representing a numerical solution to the general problem for which the exact fundamental eigenvalue is not known. A family of spherical triangles defined by the parameters $a = 0$, $b = -1$ is considered, where Θ assumes each of the four values $\pi/2$, π, $3\pi/2$, and 2π. The oblique plane defining the non-meridional side of the spherical triangles, as given by equation (7c), is $z = -y$, and this plane forms an angle of $\pi/4$ with the equator. The great circle determined by this oblique plane intersects the equator at $\theta = 0$, π, and 2π, and the interior domains of the spherical triangles appear as shown in Figure 5. As in the results discussed previously, a standard set of values for the rectangular grid parameters and constant grid spacing defined by $\gamma = 1$ are utilized. In three of the four Θ cases displayed in Table 6, the convergence of the calculated values of λ to an unknown exact fundamental eigenvalue is monotonically increasing with the refinement in grids, but in the anomalous $\Theta = \pi$ case, oscillatory behavior in the calculated values of λ is observed. No explanation for this lack of monotonicity is offered here, but this phenomenon has been observed elsewhere (Reference 6, pp. 351-352) in the numerical calculation of fundamental eigenvalues. Furthermore, in the cases $\Theta = 3\pi/2$ and $\Theta = 2\pi$, although the convergence shown is monotonic, it certainly is not uniform to the extent generally seen in earlier results for the known solution special cases.

Table 6
Fundamental Eigenvalues of Oblique Spherical Triangles (a=0,b=-1)
Using Constant Grid Spacing in the ϕ-Direction ($\gamma = 1$)

Spherical Triangle Parameter Θ	Rectangular Grid Parameters		Calculated Fundamental Eigenvalue λ	Optimal Scalar Relaxation Factor ω	Required Number of Outer Iterations m	Required Number of Gauss-Seidel Inner Iterations k_1	Required Number of S.O.R. Inner Iterations at Convergence k_m
	N_θ	N_ϕ					
$\pi/2$	10	10	7.392	1.520	8	100	28
$\pi/2$	20	20	7.569	1.731	10	100	49
$\pi/2$	30	30	7.633	1.809	11	100	77
$\pi/2$	40	40	7.668	1.854	11	150	100
π	10	10	2.795	1.519	6	100	28
π	20	20	3.027	1.724	7	100	52
π	30	30	3.000	1.823	8	100	76
π	40	40	3.061	1.843	8	150	118
$3\pi/2$	10	10	2.435	1.476	8	90	24
$3\pi/2$	20	20	2.615	1.697	7	100	47
$3\pi/2$	30	30	2.631	1.796	8	100	66
$3\pi/2$	40	40	2.664	1.844	8	150	88
2π	10	10	2.396	1.435	8	73	22
2π	20	20	2.581	1.665	8	100	42
2π	30	30	2.597	1.771	8	100	57
2π	40	40	2.652	1.811	9	100	92

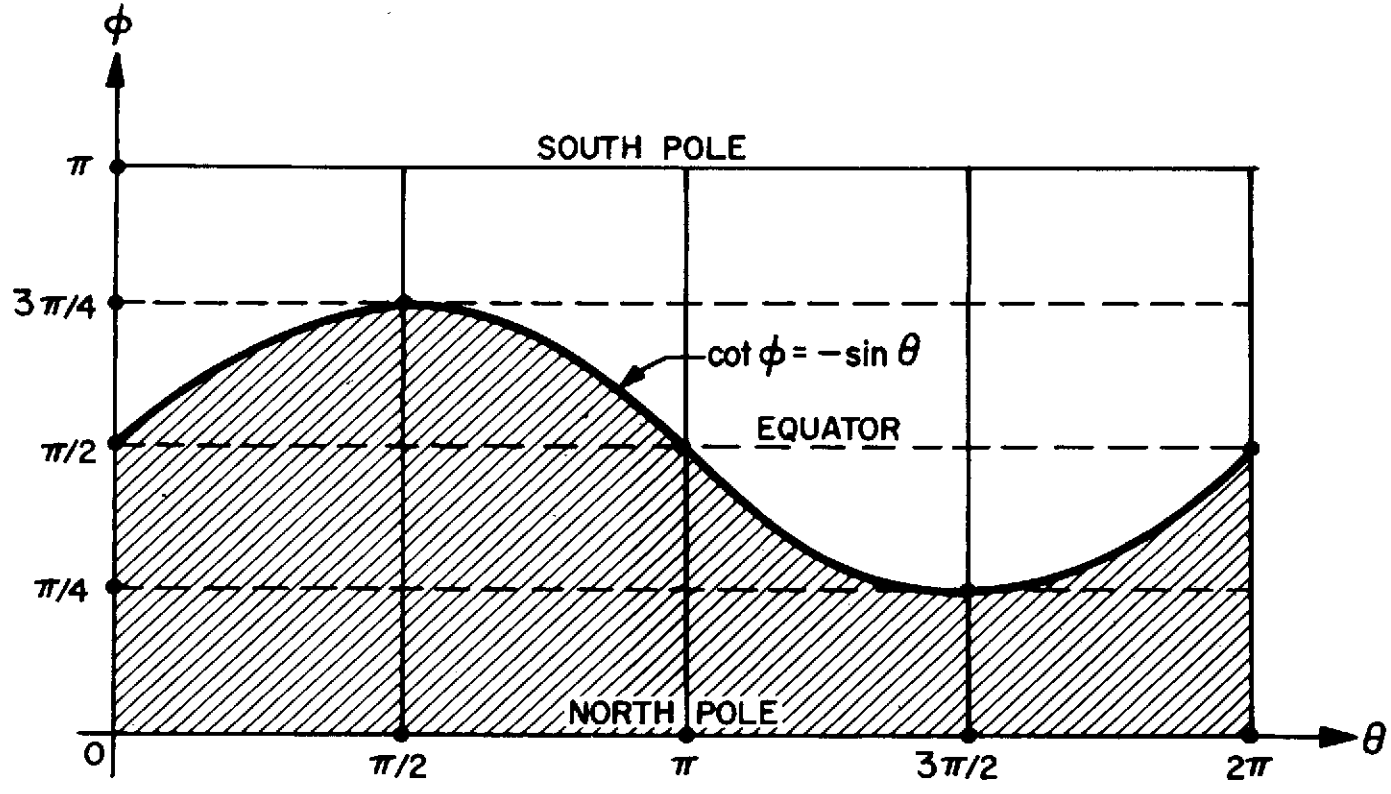

Figure 5. Interior domains of oblique spherical triangles defined by the parametric values a = 0, b = -1; $\Theta = \pi/2, \pi, 3\pi/2$, and 2π (indicated by the shaded regions to the left of each of the four respective $\theta = \Theta$ values)

The non-uniform convergence of Table 6 may well be due to the fact that the oblique spherical triangles contain a boundary great circle arc which appears as a transcendental curve in the two-dimensional θ, ϕ-plane (see Figure 5). In the general problem, this transcendental curve will be present, although it did not appear in the earlier results of this section for the special cases when all spherical surface boundaries coincided with constant-value θ and ϕ great circle arcs (i.e., lines of spherical longitude and latitude). The presence of a curved boundary in the θ, ϕ-plane requires that a series of straight line segments connecting appropriate grid points θ_i, ϕ_j be utilized to approximate the southern boundary of the spherical triangle. As the grid parameters N_θ, N_ϕ are changed, the precise location of the approximate triangle boundary varies. This could perhaps explain the non-uniform convergence in the calculated values of λ. The convergence characteristics of the relaxation factor ω and the required numbers of iterations as shown in Table 6 are similar to those noted in the earlier results for the special cases.

SECTION VI

PROBLEM OF A SPHERICAL SURFACE WITH A SLIT

A. The Slit Domain

In this section, the problem of determining the fundamental eigenvalue for a domain which is the exterior of a spherical "triangle" in the degenerate case of $\Theta = 0$ will be considered. In such a limiting case, the triangle degenerates to a meridional great circle arc or "slit." This problem is the second of the two cases mentioned in the introductory section for which the second-order elliptic partial differential equation (12) will be solved by approximation methods, with the boundary conditions supplied by equation (11b).

The slit domain D may be specified by a single slit extension parameter which shall be denoted Φ, where $0 < \Phi < \pi$. The slit may be readily placed in a canonical position so that it extends from the spherical north pole (intersection of the z-axis with the unit sphere, as previously) southward along the arc of a great circle. In terms of the spherical triangle parameters utilized previously, the value for Φ may be determined from equation (8) by setting $\Theta = 0$ (hence $\theta = 0$) so that the resulting value ϕ is equal to Φ. It is then seen that $\Phi = \operatorname{arccot} a = \arcsin (a^2 + 1)^{-1/2}$, with b arbitrary.

The spherical surface may be mapped directly onto the θ, ϕ-plane in the usual manner, as shown in Figure 6. Note that the domain of interest now includes the entire spherical surface, $0 \leq \phi \leq \pi$; $0 \leq \theta \leq 2\pi$. A network of grid points θ_i, ϕ_j, as defined by equation (13), is superposed over the spherical surface in the manner used previously, but now the relations between the number of grid intervals and the constant grid spacings are

$$h_\theta N_\theta = 2\pi, \tag{54a}$$

$$h_\phi N_\phi = \pi. \tag{54b}$$

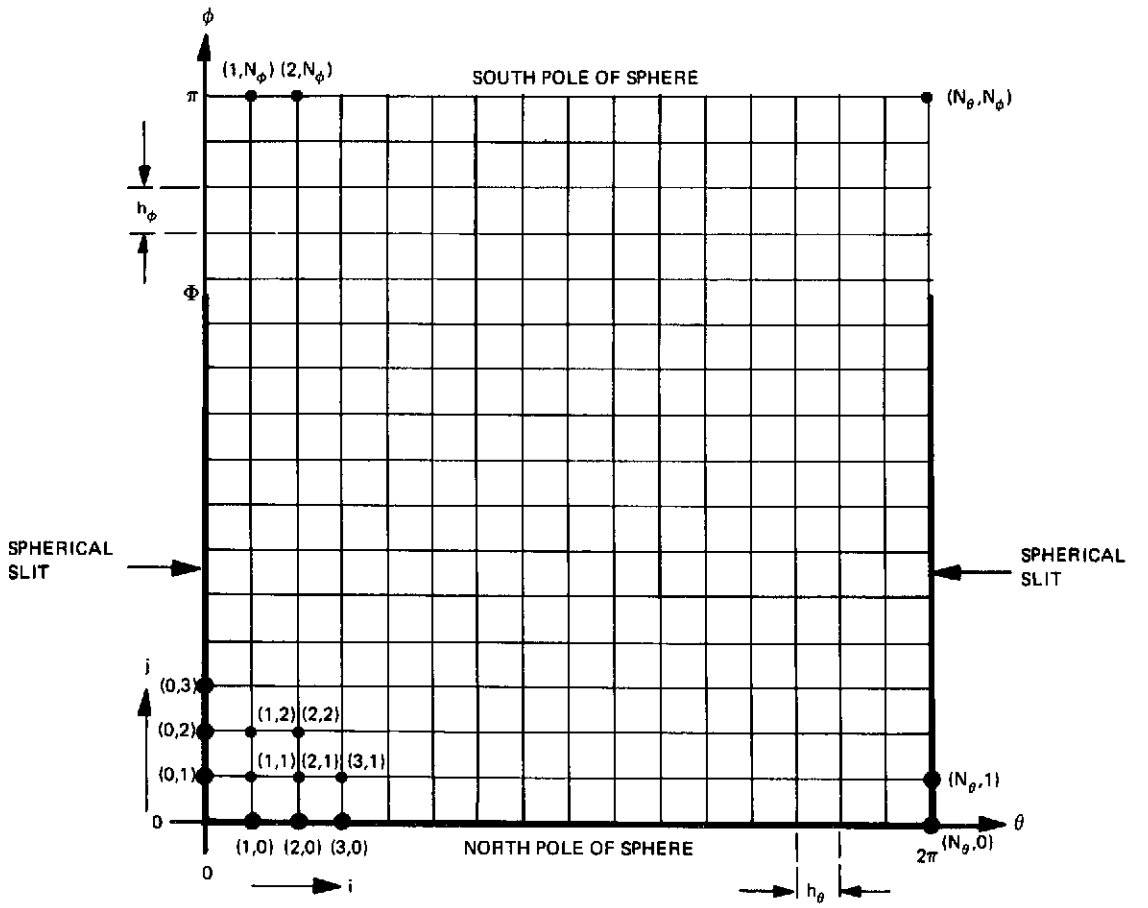

Figure 6. Network of grid points θ_i , ϕ_j superposed over entire spherical surface with a slit mapped onto a plane rectangular region

In the θ, ϕ-plane, the single slit appears along some portion of three of the rectangular boundaries, viz., the entire line representing the north pole $\phi = 0$, a portion of the line representing the slit meridian $\theta = 0$, and a like portion of the line $\theta = 2\pi$ also representing the same slit meridian. Note that, in general, the slit boundary will not terminate on a grid point.

B. Boundary Conditions

The boundary conditions (11b) to be imposed on the discretized version of the eigenvalue equation for the problem of the spherical surface with a slit may be deduced from Figure 6. They are

$$U_{i,0} = 0 \quad \text{for} \quad i = 0, 1, 2, \ldots, N_\theta, \tag{55}$$

and

$$U_{0,j} = U_{N_\theta,j} = 0 \quad \text{for} \quad j = 0, 1, 2, \ldots, N_\phi, \quad \text{if } \phi_j \leq \Phi. \tag{56}$$

The boundary conditions (55) refer to the north pole of the sphere, and the conditions (56) refer to grid points coinciding with the slit meridian boundary. Note that, in general, there are non-zero values of the grid function $U_{i,j}$ occurring along the rectangular grid boundary in Figure 6; in particular, such values may appear along the slit meridians beyond the extension of the slit (i.e., $U_{0,j}$ and $U_{N_\theta,j}$ for which $\phi_j > \Phi$) and at the south pole (i.e., U_{i,N_ϕ} for $i = 0, 1, 2, \ldots, N_\theta$). In contrast, all grid function values occurring along the rectangular grid boundary in the problem of the spherical triangle vanished. The finite difference equation (22), derived as an approximation to the continuous partial differential equation (12) for the problem of the spherical triangle, remains valid for all rectangular interior grid points (θ_i, ϕ_j), $i = 1, 2, \ldots, N_\theta - 1$; $j = 1, 2, \ldots, N_\phi - 1$ in the problem of the spherical surface with a slit. However, it must be modified in order to apply to the rectangular boundary grid points represented by the subscript values $i = 0, N_\theta$; $j = 0, 1, 2, \ldots, N_\phi$ if $\phi_j > \Phi$ and $i = 0, 1, 2, \ldots, N_\theta$; $j = N_\phi$.

Since the rectangular boundary grid points along the line $i = 0$ coincide with the respective rectangular boundary grid points along the line $i = N_\theta$ insofar as the spherical surface geometry is concerned, it is evident that the following periodic boundary conditions must be imposed in addition to conditions (55) and (56):

$$U_{0,j} = U_{N_\theta,j} \text{ for } j = 0, 1, 2, \ldots, N_\phi, \quad \text{if } \phi_j > \Phi. \tag{57}$$

In view of this periodicity, the finite difference equation (22) may be extended to the line $i = N_\theta$ by the simple device of replacing the undefined grid components $U_{N_\theta+1,j}$, $j = 0, 1, 2, \ldots, N_\phi$ by the respective defined grid components $U_{1,j}$, $j = 0, 1, 2, \ldots, N_\phi$, whenever the former occur. That is, for $i = N_\theta$, equation (22) becomes in its modified form:

$$\begin{aligned} a_j U_{N_\theta,j} - b_j U_{1,j} - c_j U_{N_\theta,j+1} - b_j U_{N_\theta-1,j} - c_{j-1} U_{N_\theta,j-1} \\ = \lambda e_j U_{N_\theta,j} \quad \text{for } j = 1, 2, \ldots, N_\phi - 1, \quad \text{if } \phi_j > \Phi, \end{aligned} \tag{58}$$

where a_j, b_j, c_j, and e_j are defined as previously. Now the finite difference equation (22) may be further extended to the line $i = 0$ merely by invoking equation (57). In order to complete the extension of the finite difference equation to the rectangular boundary grid points, it is necessary to derive relations for the grid points, U_{i,N_ϕ}, $i = 0, 1, 2, \ldots, N_\theta$, at the south pole.

C. Difference Equations at the South Pole

Difference equations pertaining to the grid points at the south pole may be derived by integrating the partial differential equation (12) over the disc $0 < \theta < 2\pi$; $\phi_{N_\phi - 1/2} < \phi < \phi_{N_\phi} = \pi$ (see Figure 7). Note that the first term on the left in equation (12) vanishes when integrated over the disc because of the 2π periodicity in the θ variable. After integrating the second term on the left in equation (12) explicitly with respect to the ϕ variable, it is seen that

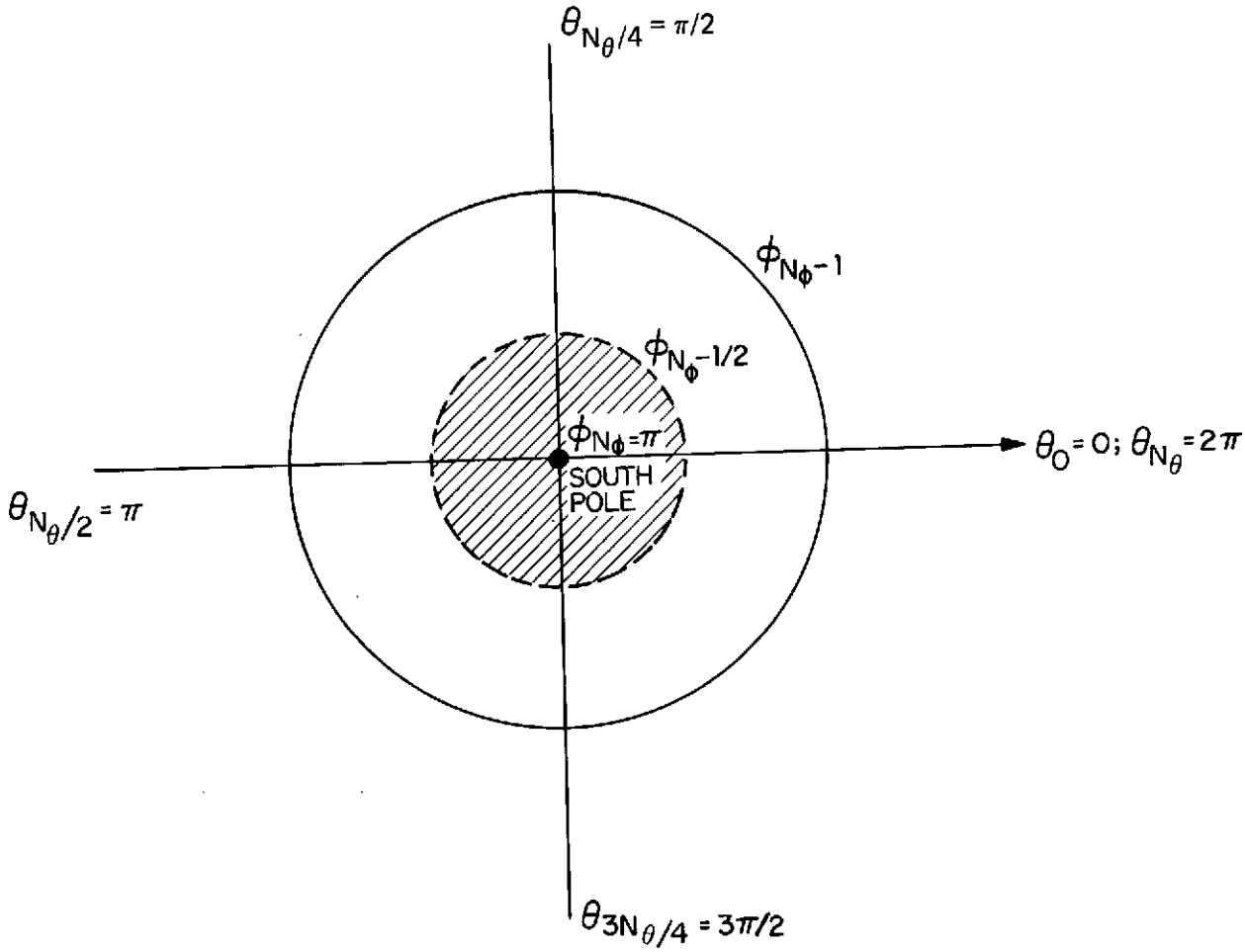

Figure 7. Disc (indicated by shading) utilized to derive difference equations valid at the spherical south pole

$$- \int_{\theta=0}^{2\pi} u_{\phi}(\theta, \phi_{N_\phi - 1/2}) \sin \phi_{N_\phi - 1/2} d\theta + \lambda \int_{\theta=0}^{2\pi} \int_{\phi_{N_\phi - 1/2}}^{\pi} u \sin \phi d\phi d\theta = 0. \tag{59}$$

The first term on the left in equation (59) may be approximated, by use of the centered first difference quotient (19), as a finite sum of the form,

$$- \sum_{i=1}^{N_\theta} \left(\frac{U_{i,N_\phi} - U_{i,N_\phi - 1}}{h_{\phi,N_\phi}} \right) h_\theta \sin \phi_{N_\phi - 1/2}. \tag{60}$$

The second term on the left in equation (59) may be approximated by

$$\lambda U_{i,N_\phi}(2\pi) \left[- \cos \phi \right] \Big|_{\phi_{N_\phi - 1/2}}^{\pi} = 2\pi\lambda U_{i,N_\phi}(1 + \cos \phi_{N_\phi - 1/2}). \tag{61}$$

In equation (61) and equations to follow, it is implicitly understood that U_{i,N_ϕ} represents the unique approximate value of the solution u at the south pole for all values of the subscript i. That is,

$$U_{1,N_\phi} = U_{i,N_\phi} \quad \text{for } i = 0, 1, 2, \ldots, N_\theta. \tag{62}$$

Now if the approximations (60) and (61) are utilized in equation (59) and the resulting equation multiplied by the factor $(2/h_\theta)$, it is seen that

$$\frac{2 \sin \phi_{N_\phi - 1/2}}{h_{\phi,N_\phi}} \sum_{i=1}^{N_\theta} (U_{i,N_\phi} - U_{i,N_\phi - 1}) = \frac{4\pi}{h_\theta} (1 + \cos \phi_{N_\phi - 1/2}) \lambda U_{i,N_\phi}. \tag{63}$$

Define the hitherto undefined quantity e_{N_ϕ} by

$$e_{N_\phi} = \frac{4\pi}{h_\theta} (1 + \cos \phi_{N_\phi - 1/2}), \tag{64}$$

which, by use of equations (54a) and (17), may be rewritten as

$$e_{N_\phi} = 2N_\theta \left(1 - \sin \frac{1}{2} \phi_{N_\phi - 1} \right) > 0. \tag{65}$$

Equation (63) may now be written, with the aid of equations (23b) and (64), as a finite difference equation for the grid points U_{i,N_ϕ} at the south pole in the form

$$c_{N_\phi - 1}\left(N_\theta U_{i,N_\phi} - \sum_{i=1}^{N_\theta} U_{i,N_\phi - 1}\right) = \lambda e_{N_\phi} U_{i,N_\phi}. \tag{66}$$

Note that the difference equation (66) is not a five-point equation, as are the difference equations (22) and (58), but is instead a $(N_\theta + 1)$-point equation. This completes the derivation of the additional finite difference equations and boundary conditions necessary to extend the solution of the problem of a spherical surface with a slit to the complete set of rectangular interior and boundary grid points.

D. Application of Successive Overrelaxation

In the matrix formulation of this problem, U represents the ordered set of unknown values $U_{i,j}$ written as a vector defined on the network of rectangular interior and boundary grid points θ_i, ϕ_j. The number of components in the vector U is equal to the number of rectangular interior grid points, $(N_\theta - 1)(N_\phi - 1)$, plus a number of rectangular boundary grid points equal to the number of grid points along either of the lines $i = 0$ or $i = N_\theta$ which do not coincide with the slit, including the single point at the south pole. This number of components of U is equal to the number of independent unknowns $U_{i,j}$ to be determined from the three finite difference equations (22), (58), and (66). Equivalently, the number of components of U is equal to the total number $(N_\theta + 1)(N_\phi + 1)$ of rectangular interior and boundary grid points reduced by the constraints of the boundary conditions at the north pole (55), along the slit (56) and its meridional extension (57), and at the south pole (62). Then the matrix form (29) of the finite difference equations, with the boundary conditions included, still applies, where A and E are now square matrices of an order equal to the dimensionality of U and with

somewhat different properties than those enumerated in the problem of the spherical triangle.

An example of the matrix formulation for the special case of $N_\theta = 4$, $N_\phi = 6$ will now be considered, where $\Phi = \pi/4$ and $\gamma = 1$ are assumed, so that constant grid spacing in the ϕ-direction results. Note that this value of Φ results in a slit boundary whose termination does not coincide with a grid point. Figure 8 displays the network of grid points, the location of the slit boundary, and a natural ordering of the grid points in which successive horizontal grid lines are scanned in order of increasing i index with the j index increasing on each new line. The rectangular boundary grid points are chosen along the line $i = N_\theta$ and the single point at the south pole is arbitrarily placed at the position $(1, N_\phi)$. The vector U in this case has dimensionality 20, of which 15 components are associated with rectangular interior grid points and the 5 remaining components with rectangular boundary grid points. Figure 9 provides the square matrix A of order 20, the square diagonal matrix E of order 20, and the vector U for this special case.

In general, the matrix A is sparse, with positive diagonal entries and non-positive off-diagonal entries. Because of the fact that the three finite difference equations (22), (58), and (66) are symmetric, the matrix A is also symmetric. However, A no longer retains the block tridiagonal property that it previously exhibited in the problem of the spherical triangle. The matrix E is diagonal with positive entries, by virtue of equations (24c) and (65). The elements of both matrices A and E depend only on the j index and are independent of i.

As an initial estimate for the power method iterations (34), $U^{(1)}$ is defined so that all components are assigned the value unity, except for the zero components associated with grid points at the north pole and along the slit boundary, in accordance with the boundary conditions (55) and (56). In particular, components

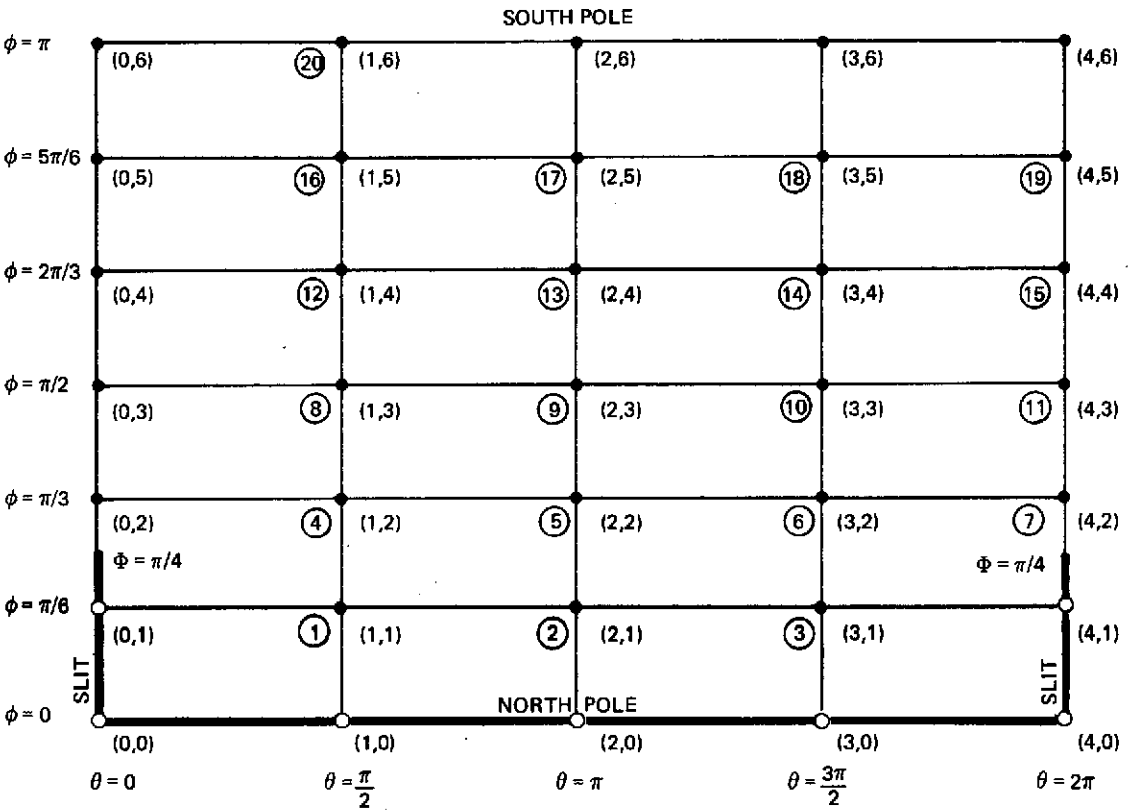

Open circles represent grid points along slit boundary (heavy line) corresponding to zero values of the grid function U.
Filled circles represent grid points corresponding to non-zero values of U.
Numbers in parentheses indicate grid point (i, j) co-ordinates.
Numbers in circles indicate natural ordering of the grid points.

Figure 8. Network of grid points for the special case $N_\theta = 4$, $N_\phi = 6$, $\Phi = \pi/4$, and $\gamma = 1$

$$
A = \begin{bmatrix}
a_1 & -b_1 & 0 & -c_1 & 0 & 0 & 0 & 0 & 0 & 0 & 0 & 0 & 0 & 0 & 0 & 0 & 0 & 0 & 0 & 0 \\
-b_1 & a_1 & -b_1 & 0 & -c_1 & 0 & 0 & 0 & 0 & 0 & 0 & 0 & 0 & 0 & 0 & 0 & 0 & 0 & 0 & 0 \\
0 & -b_1 & a_1 & 0 & 0 & -c_1 & 0 & 0 & 0 & 0 & 0 & 0 & 0 & 0 & 0 & 0 & 0 & 0 & 0 & 0 \\
-c_1 & 0 & 0 & a_2 & -b_2 & 0 & -b_2 & -c_2 & 0 & 0 & 0 & 0 & 0 & 0 & 0 & 0 & 0 & 0 & 0 & 0 \\
0 & -c_1 & 0 & -b_2 & a_2 & -b_2 & 0 & 0 & -c_2 & 0 & 0 & 0 & 0 & 0 & 0 & 0 & 0 & 0 & 0 & 0 \\
0 & 0 & -c_1 & 0 & -b_2 & a_2 & -b_2 & 0 & 0 & -c_2 & 0 & 0 & 0 & 0 & 0 & 0 & 0 & 0 & 0 & 0 \\
0 & 0 & 0 & -b_2 & 0 & -b_2 & a_2 & 0 & 0 & 0 & -c_2 & 0 & 0 & 0 & 0 & 0 & 0 & 0 & 0 & 0 \\
0 & 0 & 0 & -c_2 & 0 & 0 & 0 & a_3 & -b_3 & 0 & -b_3 & -c_3 & 0 & 0 & 0 & 0 & 0 & 0 & 0 & 0 \\
0 & 0 & 0 & 0 & -c_2 & 0 & 0 & -b_3 & a_3 & -b_3 & 0 & 0 & -c_3 & 0 & 0 & 0 & 0 & 0 & 0 & 0 \\
0 & 0 & 0 & 0 & 0 & -c_2 & 0 & 0 & -b_3 & a_3 & -b_3 & 0 & 0 & -c_3 & 0 & 0 & 0 & 0 & 0 & 0 \\
0 & 0 & 0 & 0 & 0 & 0 & -c_2 & -b_3 & 0 & -b_3 & a_3 & 0 & 0 & 0 & -c_3 & 0 & 0 & 0 & 0 & 0 \\
0 & 0 & 0 & 0 & 0 & 0 & 0 & -c_3 & 0 & 0 & 0 & a_4 & -b_4 & 0 & -b_4 & -c_4 & 0 & 0 & 0 & 0 \\
0 & 0 & 0 & 0 & 0 & 0 & 0 & 0 & -c_3 & 0 & 0 & -b_4 & a_4 & -b_4 & 0 & 0 & -c_4 & 0 & 0 & 0 \\
0 & 0 & 0 & 0 & 0 & 0 & 0 & 0 & 0 & -c_3 & 0 & 0 & -b_4 & a_4 & -b_4 & 0 & 0 & -c_4 & 0 & 0 \\
0 & 0 & 0 & 0 & 0 & 0 & 0 & 0 & 0 & 0 & -c_3 & -b_4 & 0 & -b_4 & a_4 & 0 & 0 & 0 & -c_4 & 0 \\
0 & 0 & 0 & 0 & 0 & 0 & 0 & 0 & 0 & 0 & 0 & -c_4 & 0 & 0 & 0 & a_5 & -b_5 & 0 & -b_5 & -c_5 \\
0 & 0 & 0 & 0 & 0 & 0 & 0 & 0 & 0 & 0 & 0 & 0 & -c_4 & 0 & 0 & -b_5 & a_5 & -b_5 & 0 & -c_5 \\
0 & 0 & 0 & 0 & 0 & 0 & 0 & 0 & 0 & 0 & 0 & 0 & 0 & -c_4 & 0 & 0 & -b_5 & a_5 & -b_5 & -c_5 \\
0 & 0 & 0 & 0 & 0 & 0 & 0 & 0 & 0 & 0 & 0 & 0 & 0 & 0 & -c_4 & -b_5 & 0 & -b_5 & a_5 & -c_5 \\
0 & 0 & 0 & 0 & 0 & 0 & 0 & 0 & 0 & 0 & 0 & 0 & 0 & 0 & 0 & -c_5 & -c_5 & -c_5 & -c_5 & 4c_5
\end{bmatrix}
$$

$$
U = [U_{11}U_{21}U_{31}U_{12}U_{22}U_{32}U_{42}U_{13}U_{23}U_{33}U_{43}U_{14}U_{24}U_{34}U_{44}U_{15}U_{25}U_{35}U_{45}U_{16}]^T
$$

$$
E = \mathrm{diag}[e_1 e_1 e_1 e_2 e_2 e_2 e_2 e_3 e_3 e_3 e_3 e_4 e_4 e_4 e_4 e_5 e_5 e_5 e_5 e_6]
$$

Figure 9. The square matrix A of order 20, the vector U of 20 components (the superscript "T" indicates transpose), and the square diagonal matrix E of order 20 for the special case $N_\theta = 4$, $N_\phi = 6$, $\Phi = \pi/4$, and $\gamma = 1$

associated with the grid points at the south pole and along portions of the slit meridian beyond the extension of the slit are initialized to the value unity.

The iterative method of point successive overrelaxation as applied to the finite difference equation (22) produces iterates $U^{(k)}$ whose components associated with rectangular interior grid points are given by equation (36). For values of the j index such that $\phi_j > \Phi$, the iterates $U^{(k)}$ whose components are associated with rectangular boundary grid points along the line $i = N_\theta$ are given instead by

$$U_{N_\theta, j}^{(k+1)} = \frac{\omega}{a_j} [b_j U_{1,j}^{(k+1)} + c_j U_{N_\theta, j+1}^{(k)} + b_j U_{N_\theta - 1, j}^{(k+1)} + c_{j-1} U_{N_\theta, j-1}^{(k+1)} + F_{N_\theta, j}] + (1 - \omega) U_{N_\theta, j}^{(k)}$$

$$\text{for } j = 1, 2, \ldots, N_\phi - 1, \quad \text{if } \phi_j > \Phi; \quad k = 1, 2, \ldots \tag{67}$$

The iterate components in equation (67) are, of course, based upon the finite difference equation (58). For $j = N_\phi$, the iterates $U^{(k)}$ whose component is associated with the grid points at the south pole are given by

$$U_{i, N_\phi}^{(k+1)} = \frac{\omega}{N_\theta} \left[\sum_{i=1}^{N_\theta} U_{i, N_\phi - 1}^{(k+1)} + \frac{F_{i, N_\phi}}{c_{N_\phi - 1}} \right] + (1 - \omega) U_{i, N_\phi}^{(k)}, \quad k = 1, 2, \ldots \tag{68}$$

These iterates are based upon the finite difference equation (66), and because of the uniqueness specified in equation (62), it may be seen that equation (68) is actually independent of the i index. Singularity problems do not arise, since N_θ and $c_{N_\phi - 1}$ never vanish, by definition and equation (24b), respectively. Furthermore, it is important that the iterate components given by equations (36), (67), and (68) be computed according to the natural ordering of the grid points associated with the components of the vector $U_{i,j}$. Use of the natural ordering will insure that the proper values of the superscripts k and (k+1), specifying the inner iteration number, occur automatically in the calculation process.

The vectors F that appear as k-independent constants in the inner iteration equations (67) and (68) are defined, in accordance with the finite difference equations (58) and (66), merely by extending the definition (37) in the natural way to include components associated with rectangular boundary grid points. That is, with use of definition (65),

$$F_{i,j} = e_j U_{i,j}, \quad \text{for } i = 0,\ 1,\ 2, \ldots,\ N_\theta;\quad j = 1,\ 2, \ldots,\ N_\phi. \tag{69}$$

Similarly, the definition (38a) of the convergence parameters $\epsilon^{(k)}$ must be extended to the full range of grid point indexing as follows:

$$\epsilon^{(k)} \equiv \max_{\substack{0 \le i \le N_\theta \\ 0 \le j \le N_\phi}} \left| U_{i,j}^{(k+1)} - U_{i,j}^{(k)} \right|, \quad k = 1,\ 2, \ldots \tag{70}$$

The range of the summations involved in the Rayleigh quotient (35) must likewise be adjusted to account for the proper range of grid point indexing. The vector inner products may be written in component form as $\lambda^{(m)} = P/Q$, where, in contrast to equations (42),

$$P = (U^{(m)},\ EU^{(m)}) = \sum_{i=1}^{N_\theta} \left(\sum_{j=1}^{N_\phi - 1} \frac{F_{i,j}^2}{e_j} \right) + \frac{F_{1,N_\phi}^2}{e_{N_\phi}} \tag{71a}$$

and

$$Q = (A^{-1}EU^{(m)},\ EU^{(m)}) = \sum_{i=1}^{N_\theta} \left(\sum_{j=1}^{N_\phi - 1} F_{i,j} U_{i,j} \right) + F_{1,N_\phi} U_{1,N_\phi} \tag{71b}$$

In the summations appearing in equations (71), components associated with rectangular boundary grid points along the line $i = 0$ are excluded, since such components are redundant to those along the boundary line $i = N_\theta$, the latter of which are included in the summations. Also, the single components associated with the grid points at the south pole are presented separately as the final term on the right side of equations (71). Finally, the component form (45) of the power method must be extended to the full range of grid point indexing as in the following:

$$U_{i,j}^{(m+1)} = \lambda^{(m)} U_{i,j}^{(m)}, \quad \text{for } i = 0, 1, 2, \ldots, N_\theta; \quad j = 1, 2, \ldots, N_\phi. \tag{72}$$

The theoretical demonstration of convergence of the successive overrelaxation iterates (36), (67), and (68) for any initial vector $U^{(1)}$ selected follows from the Ostrowski-Reich theorem (Reference 7, p. 123) for a relaxation factor ω in the range $0 < \omega < 2$. As stated previously in Section III, this theorem can be invoked because A may be shown to be a symmetric irreducibly diagonally dominant matrix which is, therefore, positive definite. Although the method of successive overrelaxation will converge for all relaxation factors in the above range, the most rapid convergence occurs for some optimal value ω_{opt} of ω in the interval $1 < \omega < 2$. However, since in the problem of a spherical surface with a slit, difference equations arise which are not of the five-point type, it is not true that the Jacobi matrix associated with A is cyclic of index 2, as was the case previously in the problem of the spherical triangle. This means that the theoretical expression (40) for ω_{opt} no longer applies. An expression for the actual optimal value ω_{opt} of ω is not known for the current problem. However, it has been suggested (Reference 6, p. 262) that the value of ω produced by the formula (40) may be reasonably close to the unknown optimal value ω_{opt}, even when the theoretical expression (40) does not rigorously apply. For this reason and in light of the fact that a better method for approximating the true value of ω_{opt} is not available, the formula (40), based upon the convergence (39) of parameters $r^{(k)}$ defined in equation (38b), is retained for approximating ω_{opt} in the numerical results that follow.

The implementation of the numerical technique, as previously described in Section III, for the solution of the finite difference equations by point successive overrelaxation and the subsequent iterative determination of the fundamental eigenvalue proceeds in precisely the same manner for the digital computer

solution of the problem of a spherical surface with a slit. Application of these techniques is clarified by the algorithmic presentation within Appendix B of the methods discussed in the current section. In the algorithm of Appendix B, the vector U is considered to be an array with $(N_\theta + 1)(N_\phi + 1)$ entries, so that an entry of U is associated with each rectangular interior and boundary grid point regardless of the value of the slit extension parameter Φ. From a computational standpoint, this device of enlarging the dimensionality of U, with the constraints (55), (56), (57), and (62) imposed upon the entries of the array, is merely a convenience in indexing.

E. Numerical Results

In the numerical applications to be described, the slit extension parameter Φ was assigned a range of values in the interval $0 < \Phi < \pi$ in a systematic manner, and for each such value of Φ, several rectangular grid parametric values were considered. Table 7 displays calculated values for the fundamental eigenvalue λ for each of the values $\Phi = n(\pi/8)$, $n = 1, 2, \ldots, 7$ and for the familiar gamut of rectangular grid parameters, $N_\theta = N_\phi = 10, 20, 30, 40$. All the grids utilized a grid spacing parameter $\gamma = 1$, so that uniform θ,φ-plane grid spacing resulted. The criteria for iterative convergence remain $\epsilon_{INNER} = \epsilon_{OUTER} = 10^{-6}$. The description provided in Section V of the significance of the various columns within the tables applies equally well to Table 7. The value for the increment Δk_{max} used to promote inner convergence when the current value of k_{max} is not sufficient remains at 50, as previously.

The significant results provided by Table 7 include the qualitative fact that the calculated value of λ increases with the extent of the spherical slit as measured by Φ. However, the convergence in λ with increasing rectangular grid parameters for a given Φ is by no means monotonic, as generally was the case in the problem of the spherical triangle. The calculated values for the

Table 7

Fundamental Eigenvalues of a Spherical Surface with a Slit

Spherical Slit Extension Parameter Φ	Rectangular Grid Parameters		Calculated Fundamental Eigenvalue λ	Near-Optimal Scalar Relaxation Factor ω	Required Number of Outer Iterations m	Required Number of Gauss-Seidel Inner Iterations k_1	Required Number of S.O.R. Inner Iterations at Convergence k_m
	N_θ	N_ϕ					
$\pi/8$	10	10	0.209	1.794	4	100	90
$\pi/8$	20	20	0.193	1.900	4	200	195
$\pi/8$	30	30	0.188	1.937	5	300	283
$\pi/8$	40	40	0.199	1.960	5	400	317
$\pi/4$	10	10	0.263	1.773	4	100	80
$\pi/4$	20	20	0.273	1.883	5	200	164
$\pi/4$	30	30	0.259	1.926	5	250	245
$\pi/4$	40	40	0.265	1.953	5	350	271
$3\pi/8$	10	10	0.317	1.755	5	100	73
$3\pi/8$	20	20	0.325	1.874	5	200	150
$3\pi/8$	30	30	0.327	1.917	5	250	223
$3\pi/8$	40	40	0.329	1.949	5	300	242
$\pi/2$	10	10	0.427	1.722	5	100	61
$\pi/2$	20	20	0.406	1.860	5	150	133
$\pi/2$	30	30	0.399	1.910	5	200	198
$\pi/2$	40	40	0.396	1.941	5	300	229
$5\pi/8$	10	10	0.486	1.705	5	100	56
$5\pi/8$	20	20	0.465	1.851	5	150	122
$5\pi/8$	30	30	0.457	1.905	5	200	180
$5\pi/8$	40	40	0.469	1.936	5	300	203
$3\pi/4$	10	10	0.550	1.688	5	100	51
$3\pi/4$	20	20	0.563	1.835	5	150	104
$3\pi/4$	30	30	0.544	1.884	5	200	182
$3\pi/4$	40	40	0.551	1.897	6	300	295
$7\pi/8$	10	10	0.619	1.668	6	100	46
$7\pi/8$	20	20	0.637	1.811	6	100	100
$7\pi/8$	30	30	0.644	1.860	6	200	169
$7\pi/8$	40	40	0.647	1.880	6	300	262

"near-optimal" scalar relaxation factor ω do increase monotonically with the refinement in the grid, and it is also observed that for a fixed pair of rectangular grid parameters, the calculated ω increases progressively as Φ decreases. A similar monotonic increase in the required number of inner and outer iterations occurs with the grid refinement for each value of Φ. Note also that for a fixed pair of N_θ, N_ϕ values, the required number k_m of inner iterations at convergence increases dramatically as Φ decreases. A parallel phenomenon is seen for the required number k_1 of Gauss-Seidel inner iterations for the first outer iterations. The change in the required number m of outer iterations, although a much more moderate variance, exhibits a reverse trend, viz., a slight decrease with the decrease in Φ . In sum, these results indicate that convergence in λ occurs more slowly (1) for a finer grid than for a coarse grid, and (2) as the slit extension decreases toward the north pole. Also, in comparison with the results for the problem of the spherical triangle, the Table 7 results indicate that convergence in λ to the 10^{-6} criteria requires a substantially greater number of inner iterations and a moderately smaller number of outer iterations. The slower convergence of the successive overrelaxation method for the problem of a spherical surface with a slit is no doubt due to the fact that an expression for the optimal value of ω is not available, as explained previously.

A further investigation was conducted to determine the effects of utilizing values of Φ near the polar limits of 0 and π for the slit boundary. The results appear in Table 8. It was desirable to choose two values, Φ_1 and Φ_2, such that $0 < \Phi_1 < \pi/40$ and $\pi - (\pi/40) < \Phi_2 < \pi$ in order that none of the grid points, except those at the north pole, would coincide with the slit boundary (in the case of Φ_1) and in order that all of the grid points along the slit meridian, except those at the south pole, would coincide with the slit boundary (in the case of Φ_2), for all values of the rectangular grid parameters, $N_\theta = N_\phi = 10, 20, 30, 40$. The values arbitrarily adopted that meet these criteria were $\Phi_1 = \pi/100$ and $\Phi_2 = 99\pi/100$.

Table 8
Fundamental Eigenvalues of a Spherical Surface with a Slit
Near Slit Boundary Polar Limiting Values

Spherical Slit Extension Parameter Φ	Rectangular Grid Parameters		Calculated Fundamental Eigenvalue λ	Near-Optimal Scalar Relaxation Factor ω	Required Number of Outer Iterations m	Required Number of Gauss-Seidel Inner Iterations k_1	Required Number of S.O.R. Inner Iterations at Convergence k_m
	N_θ	N_ϕ					
$\pi/100$	10	10	0.147	1.825	4	150	110
$\pi/100$	20	20	0.123	1.919	4	250	249
$\pi/100$	30	30	0.112	1.950	4	400	383
$\pi/100$	40	40	0.105	1.971	4	500	459
$99\pi/100$	10	10	0.697	1.646	6	100	40
$99\pi/100$	20	20	0.724	1.790	6	100	87
$99\pi/100$	30	30	0.733	1.843	6	200	143
$99\pi/100$	40	40	0.737	1.863	6	300	222

The calculated fundamental eigenvalues display a monotonic decrease for $\Phi = \pi/100$ and a monotonic increase for $\Phi = 99\pi/100$, with the refinement in grids. More significantly, the calculated λ values are in accordance with the trend noted in the Table 7 results, i.e., λ increases with Φ. In addition, all the characteristics noted in the results of Table 7 for the scalar relaxation factor ω and the required numbers of outer and inner iterations m, k_1, and k_m are exhibited further by the results of Table 8. In particular, the slow convergence of the inner iterations for $\Phi = \pi/100$ and the correspondingly rapid convergence of the inner iterations for $\Phi = 99\pi/100$ are emphasized in the Table 8 results.

Finally, the value of the calculated fundamental eigenvalue as a function of the spherical slit extension parameter is graphically displayed for three of the rectangular grids in Figure 10 (the case $N_\theta = N_\phi = 30$ is omitted from the figure for purposes of legibility only). It is seen that λ versus Φ is a very nearly linear relationship, with a slope $d\lambda/d\Phi$ of approximately 0.2 per radian. It will be recalled that the special case of a spherical surface with a slit parameter $\Phi = \pi$ was solved analytically in Section IV as a limiting case for a spherical wedge-shaped domain. The exact value for the fundamental eigenvalue was analytically found to be $\lambda = 3/4$. The results in Table 8 for $\Phi = 99\pi/100$, which are included in Figure 10, are in excellent agreement with this theoretical result. It is also noted from Figure 10, and the results in Table 8 for $\Phi = \pi/100$, that the limiting value as Φ approaches zero (and the spherical surface with a slit degenerates to a sphere with a boundary point at the north pole) tends rather slowly to the true value $\lambda = 0$, with the refinement in the rectangular grids. Further experiments conducted with still finer grids in which $N_\phi > 40$ indicated that this convergence of the fundamental eigenvalue toward zero did indeed proceed, albeit quite gradually.

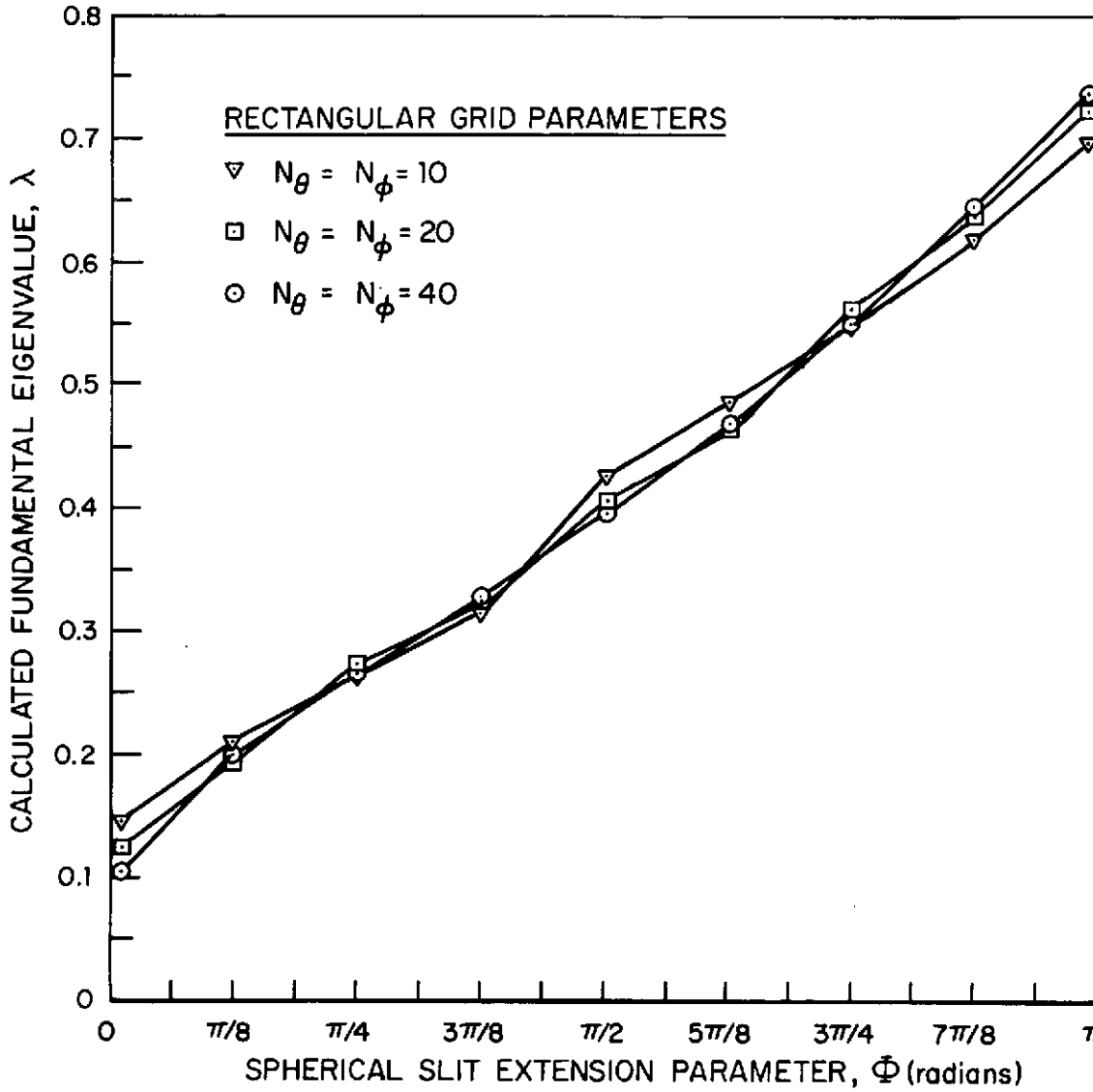

Figure 10. The value of the calculated fundamental eigenvalue λ as a function of the spherical slit extension parameter Φ for various rectangular grids (N_θ by N_ϕ intervals)

REFERENCES

1. Kellogg, R. B., "Singularities in Interface Problems," pp. 351-400 in Numerical Solution of Partial Differential Equations-II, edited by Bert Hubbard, New York and London: Academic Press, 1971.

2. Courant, R. and Hilbert, D., Methods of Mathematical Physics, Volume I, New York: Interscience Publishers, 1953.

3. Carnahan, Brice, Luther, H. A., and Wilkes, James O., Applied Numerical Methods, New York and London: John Wiley & Sons, 1969.

4. Varga, Richard S., Matrix Iterative Analysis, Englewood Cliffs, N. J.: Prentice-Hall, 1962.

5. Isaacson, Eugene and Keller, Herbert B., Analysis of Numerical Methods, New York and London: John Wiley & Sons, 1966.

6. Forsythe, George E. and Wasow, Wolfgang R., Finite-Difference Methods for Partial Differential Equations, New York and London: John Wiley & Sons, 1960.

7. Ortega, James M., Numerical Analysis: A Second Course, New York and London: Academic Press, 1972.

APPENDIX A

ALGORITHM FOR CALCULATING THE FUNDAMENTAL EIGENVALUE OF A SPHERICAL TRIANGLE

1. The following parameters are given initially:

a. the spherical triangle parameters, Θ, a, b, (7)*

where $0 < \Theta \leq 2\pi$, $-\infty < a, b < \infty$;

b. the rectangular grid parameters, N_θ, N_ϕ, (13)

where both N_θ and N_ϕ are positive integers greater than unity, and, in the general case, N_ϕ must be an even integer;

c. the parameter, γ, defining the grid spacing in the ϕ-direction, where γ is positive; (28)

d. the criteria, ϵ_{INNER}, ϵ_{OUTER}, for iterative convergence, where $0 < \epsilon_{INNER}, \epsilon_{OUTER} << 1$; and (41)

e. the upper limits, k_{max}, m_{max}, on the number of iterations permitted for inner and outer convergence, respectively, where both k_{max} and m_{max} are positive integers.

2. Calculate the grid spacing in the θ-direction:

$$h_\theta = \frac{\Theta}{N_\theta}. \tag{14a}$$

3. Calculate the following vector components as constant parameters for the iterative procedure:

$$\left.\begin{aligned} \theta_i &= i h_\theta \\ M_i &= a \cos\theta_i + b \sin\theta_i \end{aligned}\right\} \text{ for } i = 1, 2, \ldots, N_\theta - 1 \tag{13}$$

$$\left.\begin{aligned} \phi_j &= \left(\frac{2j}{N_\phi}\right)^\gamma \frac{\pi}{2} \\ \phi_{N_\phi - j} &= \pi - \phi_j \end{aligned}\right\} \text{ for } j = 0, 1, 2, \ldots, \frac{1}{2}N_\phi \tag{28}$$

*These equation numbers provide a reference to the discussion in the main body of the text.

Note: If $\gamma = 1$, then the above calculations reduce to

$$\phi_j = \frac{j\pi}{N_\phi} \quad \text{for } j = 0, 1, 2, \ldots, N_\phi, \tag{13; 14b}$$

and N_ϕ may be any positive integer greater than unity (not necessarily even).

$$\left.\begin{aligned} N_j &= \cot \phi_j \\ b_j &= \frac{\phi_{j+1} - \phi_{j-1}}{h_\theta^2 \sin \phi_j} \end{aligned}\right\} \text{for } j = 1, 2, \ldots, N_\phi - 1 \tag{24a}$$

$$c_j = \frac{2 \sin \frac{1}{2}(\phi_j + \phi_{j+1})}{\phi_{j+1} - \phi_j} \quad \text{for } j = 0, 1, 2, \ldots, N_\phi - 1 \tag{24b}$$

$$\left.\begin{aligned} e_j &= (\phi_{j+1} - \phi_{j-1}) \sin \phi_j \qquad (24c) \\ a_j &= 2b_j + c_j + c_{j-1} \qquad (23d) \end{aligned}\right\} \text{for } j = 1, 2, \ldots, N_\phi - 1$$

4. Impose the boundary conditions:

$$\left.\begin{aligned} U_{0,j} &= 0 \\ U_{N_\theta, j} &= 0 \end{aligned}\right\} \text{for } j = 0, 1, 2, \ldots, N_\phi \tag{25}$$

$$\left.\begin{aligned} U_{i,0} &= 0 \\ U_{i,N_\phi} &= 0 \end{aligned}\right\} \text{for } i = 0, 1, 2, \ldots, N_\theta \tag{27}$$

5. Initialize U for the power method:

$$\left.\begin{aligned} &\text{if } (M_i - N_j) \geq 0, \text{ then } U_{i,j} = 0; \\ &\text{if } (M_i - N_j) < 0, \text{ then } U_{i,j} = 1 \end{aligned}\right\} \begin{aligned} &\text{for } i = 1, 2, \ldots, N_\theta - 1; \\ &\quad j = 1, 2, \ldots, N_\phi - 1. \end{aligned} \tag{26}$$

6. Initialize the outer iteration index (set m = 1) and initialize the scalar relaxation factor (set $\omega = 1$) for Gauss-Seidel iteration.

7. Calculate:

$$F_{i,j} = e_j U_{i,j} \quad \text{for } i = 1, 2, \ldots, N_\theta - 1; \quad j = 1, 2, \ldots, N_\phi - 1. \tag{37}$$

8. Initialize the inner iteration index (set k = 0).

9. Increase the value of the inner iteration index by unity, i.e., replace k by (k + 1). Also, initialize the convergence parameter $\epsilon^{(k)}$ by equating it to zero.

10. Begin the iterative successive overrelaxation process:

$$\text{if } (M_i - N_j) \geq 0, \quad \text{then } U_{i,j}^{(k+1)} = 0;$$

$$\text{if } (M_i - N_j) < 0, \quad \text{then}$$

$$U_{i,j}^{(k+1)} = \frac{\omega}{a_j} [b_j U_{i+1,j}^{(k)} + c_j U_{i,j+1}^{(k)} + b_j U_{i-1,j}^{(k+1)} + c_{j-1} U_{i,j-1}^{(k+1)} + F_{i,j}] + (1 - \omega) U_{i,j}^{(k)}, \tag{36}$$

for $i = 1, 2, \ldots, N_\theta - 1$; $j = 1, 2, \ldots, N_\phi - 1$.

For each i, j in this range,

$$\text{if } |U_{i,j}^{(k+1)} - U_{i,j}^{(k)}| > \epsilon^{(k)}, \quad \text{then set } \epsilon^{(k)} = |U_{i,j}^{(k+1)} - U_{i,j}^{(k)}|;$$

otherwise, do not change the current value of $\epsilon^{(k)}$. This procedure determines

$$\epsilon^{(k)} = \max_{\substack{1 \leq i \leq N_\theta - 1 \\ 1 \leq j \leq N_\phi - 1}} |U_{i,j}^{(k+1)} - U_{i,j}^{(k)}|. \tag{38a}$$

11. If $k \geq 2$, then calculate the convergence parameter

$$r^{(k)} = \epsilon^{(k)} / \epsilon^{(k-1)}. \tag{38b}$$

In the case k = 1, omit this calculation.

12. If $\epsilon^{(k)} \geq \epsilon_{INNER}$ and $k \geq k_{max}$, then the inner iterations do not converge within the allotted number of iterations. If m = 1, disregard such non-convergence and proceed to step 13. However, if m > 1, the algorithm does not converge to the desired eigenvalue. Return to step 1.

If $\epsilon^{(k)} \geq \epsilon_{INNER}$ and $k < k_{max}$, then continue the inner iterations by returning to step 9.

If $\epsilon^{(k)} < \epsilon_{INNER}$, then the inner iterations have converged. Proceed to step 13.

13. Calculate the approximate fundamental eigenvalue by the Rayleigh quotient:

$$P = \sum_{i=1}^{N_\theta - 1} \left(\sum_{j=1}^{N_\phi - 1} \frac{F_{i,j}^2}{e_j} \right) \tag{42a}$$

$$Q = \sum_{i=1}^{N_\theta - 1} \left(\sum_{j=1}^{N_\phi - 1} F_{i,j} U_{i,j} \right) \tag{42b}$$

$$\lambda^{(m)} = P/Q.$$

14. If $m = 1$, proceed to step 15.

If $m > 1$ and if $|\lambda^{(m)} - \lambda^{(m-1)}| < \epsilon_{OUTER}$ as in inequality (43), then the outer iterations have converged, and $\lambda^{(m)}$ is the calculated fundamental eigenvalue. The numerical solution is completed.

If $m > 1$ and if $|\lambda^{(m)} - \lambda^{(m-1)}| \geq \epsilon_{OUTER}$ as in inequality (44), then if $m \geq m_{max}$, the outer iterations do not converge within the allotted number of iterations. The algorithm in this case does not converge to the desired eigenvalue. Return to step 1.

If $m > 1$ and if $|\lambda^{(m)} - \lambda^{(m-1)}| \geq \epsilon_{OUTER}$, but if $m < m_{max}$, then continue the outer iterations by proceeding to step 15.

15. Re-initialize U for successive overrelaxation by the power method:

$$U_{i,j}^{(m+1)} = \lambda^{(m)} U_{i,j}^{(m)} \quad \text{for} \quad i = 1, 2, \ldots, N_\theta - 1; \quad j = 1, 2, \ldots, N_\phi - 1. \tag{45}$$

If $m = 1$ (and assuming that $r^{(k)} \leq 1$), then compute an optimal scalar relaxation factor by

$$\omega = \frac{2}{1 + \sqrt{1 - r^{(k)}}}. \tag{40}$$

If $m > 1$, omit this calculation.

Increase the value of the outer iteration index by unity, i.e., replace m by $(m + 1)$, and resume successive overrelaxation by returning to step 7.

APPENDIX B

ALGORITHM FOR CALCULATING THE FUNDAMENTAL EIGENVALUE OF A SPHERICAL SURFACE WITH A SLIT

1. The following parameters are given initially:

   a. the slit extension parameter, Φ, where $0 < \Phi < \pi$;

   b. the rectangular grid parameters, N_θ, N_ϕ, (13)*
   where both N_θ and N_ϕ are positive integers greater than unity, and, in the general case, N_ϕ must be an even integer;

   c. the parameter, γ, defining the grid spacing in the ϕ-direction, where γ is positive; (28)

   d. the criteria, ϵ_{INNER}, ϵ_{OUTER}, for iterative convergence, where $0 < \epsilon_{INNER}$, $\epsilon_{OUTER} << 1$; and (41)

   e. the upper limits, k_{max}, m_{max}, on the number of iterations permitted for inner and outer convergence, respectively, where both k_{max} and m_{max} are positive integers.

2. Calculate the grid spacing in the θ-direction:

$$h_\theta = \frac{2\pi}{N_\theta}. \tag{54a}$$

3. Calculate the following vector components as constant parameters for the iterative procedure:

$$\left.\begin{aligned} \phi_j &= \left(\frac{2j}{N_\phi}\right)^\gamma \frac{\pi}{2} \\ \phi_{N_\phi - j} &= \pi - \phi_j \end{aligned}\right\} \text{ for } j = 0,\ 1,\ 2, \ldots,\ \frac{1}{2}N_\phi. \tag{28}$$

*These equation numbers provide a reference to the discussion in the main body of the text.

Note: If $\gamma = 1$, then the above calculations reduce to

$$\phi_j = \frac{j\pi}{N_\phi} \quad \text{for } j = 0, 1, 2, \ldots, N_\phi, \tag{13; 54b}$$

and N_ϕ may be any positive integer greater than unity (not necessarily even).

$$b_j = \frac{\phi_{j+1} - \phi_{j-1}}{h_\theta^2 \sin \phi_j} \quad \text{for } j = 1, 2, \ldots, N_\phi - 1 \tag{24a}$$

$$c_j = \frac{2 \sin \frac{1}{2}(\phi_j + \phi_{j+1})}{\phi_{j+1} - \phi_j} \quad \text{for } j = 0, 1, 2, \ldots, N_\phi - 1 \tag{24b}$$

$$\left.\begin{aligned} e_j &= (\phi_{j+1} - \phi_{j-1}) \sin \phi_j \\ a_j &= 2b_j + c_j + c_{j-1} \end{aligned}\right\} \quad \text{for } j = 1, 2, \ldots, N_\phi - 1 \qquad \begin{matrix} (24c) \\ (23d) \end{matrix}$$

$$e_{N_\phi} = 2N_\theta \left(1 - \sin \frac{1}{2}\phi_{N_\phi - 1}\right) \tag{65}$$

4. Impose the boundary conditions:

$$U_{i,0} = 0 \quad \text{for} \quad i = 0, 1, 2, \ldots, N_\theta \tag{55}$$

$$\left.\begin{aligned} U_{0,j} &= 0 \\ U_{N_\theta, j} &= 0 \end{aligned}\right\} \quad \text{for } j = 0, 1, 2, \ldots, N_\phi, \text{ if } \phi_j \leq \Phi. \tag{56}$$

5. Initialize U for the power method:

$$U_{i,j} = 1 \quad \text{for} \quad i = 1, 2, \ldots, N_\theta - 1; \quad j = 1, 2, \ldots, N_\phi$$

$$\left.\begin{aligned} U_{0,j} &= 1 \\ U_{N_\theta, j} &= 1 \end{aligned}\right\} \quad \text{for } j = 1, 2, \ldots, N_\phi, \text{ if } \phi_j > \Phi.$$

6. Initialize the outer iteration index (set m = 1) and initialize the scalar relaxation factor (set $\omega = 1$) for Gauss-Seidel iteration.

7. Calculate:

$$F_{i,j} = e_j U_{i,j} \quad \text{for} \quad i = 0, 1, 2, \ldots, N_\theta; \quad j = 1, 2, \ldots, N_\phi. \tag{69}$$

8. Initialize the inner iteration index (set k = 0).

9. Increase the value of the inner iteration index by unity, i.e., replace k by (k+1). Also, initialize the convergence parameter $\epsilon^{(k)}$ by equating it to zero.

10. Begin the iterative successive overrelaxation process:

$$U_{i,j}^{(k+1)} = \frac{\omega}{a_j} [b_j U_{i+1,j}^{(k)} + c_j U_{i,j+1}^{(k)} + b_j U_{i-1,j}^{(k+1)} + c_{j-1} U_{i,j-1}^{(k+1)} + F_{i,j}] + (1 - \omega) U_{i,j}^{(k)}, \tag{36}$$

$$\text{for } i = 1, 2, \ldots, N_\theta - 1; \; j = 1, 2, \ldots, N_\phi - 1.$$

Following the above computation for $i = N_\theta - 1$; j, compute:

$$U_{N_\theta,j}^{(k+1)} = \frac{\omega}{a_j} [b_j U_{1,j}^{(k+1)} + c_j U_{N_\theta,j+1}^{(k)} + b_j U_{N_\theta-1,j}^{(k+1)} + c_{j-1} U_{N_\theta,j-1}^{(k+1)} + F_{N_\theta,j}] + (1 - \omega) U_{N_\theta,j}^{(k)}$$

$$\text{for } j = 1, 2, \ldots, N_\phi - 1, \quad \text{if } \phi_j > \Phi; \tag{67}$$

$$U_{0,j}^{(k+1)} = U_{N_\theta,j}^{(k+1)} \quad \text{for } j = 1, 2, \ldots, N_\phi - 1, \quad \text{if } \phi_j > \Phi. \tag{57}$$

Now proceed with the computations (36), interspersing the computations (67) and (57) as necessary.

Upon completion of the computations (36), compute:

$$U_{i,N_\phi}^{(k+1)} = \frac{\omega}{N_\theta} \left[\sum_{\ell=1}^{N_\theta} U_{\ell,N_\phi-1}^{(k+1)} + \frac{F_{i,N_\phi}}{c_{N_\phi-1}} \right] + (1 - \omega) U_{i,N_\phi}^{(k)}, \tag{68}$$

for $i = 0, 1, 2, \ldots, N_\theta$.

For each $i = 0, 1, 2, \ldots, N_\theta$; $j = 0, 1, 2, \ldots, N_\phi$, if $|U_{i,j}^{(k+1)} - U_{i,j}^{(k)}| > \epsilon^{(k)}$, then set $\epsilon^{(k)} = |U_{i,j}^{(k+1)} - U_{i,j}^{(k)}|$; otherwise, do not change the current value of $\epsilon^{(k)}$. This procedure determines

$$\epsilon^{(k)} = \max_{\substack{0 \le i \le N_\theta \\ 0 \le j \le N_\phi}} |U_{i,j}^{(k+1)} - U_{i,j}^{(k)}|. \tag{70}$$

11. If $k \geq 2$, then calculate the convergence parameter

$$r^{(k)} = \epsilon^{(k)}/\epsilon^{(k-1)}. \tag{38b}$$

In the case $k = 1$, omit this calculation.

12. If $\epsilon^{(k)} \geq \epsilon_{INNER}$ and $k \geq k_{max}$, then the inner iterations do not converge within the allotted number of iterations. If $m = 1$, disregard such non-convergence and proceed to step 13. However, if $m > 1$, the algorithm does not converge to the desired eigenvalue. Return to step 1.

If $\epsilon^{(k)} \geq \epsilon_{INNER}$ and $k < k_{max}$, then continue the inner iterations by returning to step 9.

If $\epsilon^{(k)} < \epsilon_{INNER}$, then the inner iterations have converged. Proceed to step 13.

13. Calculate the approximate fundamental eigenvalue by the Rayleigh quotient:

$$P = \sum_{i=1}^{N_\theta} \left(\sum_{j=1}^{N_\phi - 1} \frac{F_{i,j}^2}{e_j} \right) + \frac{F_{1,N_\phi}^2}{e_{N_\phi}} \tag{71a}$$

$$Q = \sum_{i=1}^{N_\theta} \left(\sum_{j=1}^{N_\phi - 1} F_{i,j} U_{i,j} \right) + F_{1,N_\phi} U_{1,N_\phi} \tag{71b}$$

$$\lambda^{(m)} = P/Q.$$

14. If $m = 1$, proceed to step 15.

If $m > 1$ and if $|\lambda^{(m)} - \lambda^{(m-1)}| < \epsilon_{OUTER}$ as in inequality (43), then the outer iterations have converged, and $\lambda^{(m)}$ is the calculated fundamental eigenvalue. The numerical solution is completed.

If $m > 1$ and if $|\lambda^{(m)} - \lambda^{(m-1)}| \geq \epsilon_{OUTER}$ as in inequality (44), then if $m \geq m_{max}$, the outer iterations do not converge within the allotted number of iterations. The algorithm in this case does not converge to the desired eigenvalue. Return to step 1.

If $m > 1$ and if $|\lambda^{(m)} - \lambda^{(m-1)}| \geq \epsilon_{OUTER}$, but if $m < m_{max}$, then continue the outer iterations by proceeding to step 15.

15. Re-initialize U for successive overrelaxation by the power method:

$$U_{i,j}^{(m+1)} = \lambda^{(m)} U_{i,j}^{(m)} \quad \text{for } i = 0, 1, 2, \ldots, N_\theta; \quad j = 1, 2, \ldots, N_\phi. \tag{72}$$

If m = 1 (and assuming that $r^{(k)} \leq 1$), then compute a scalar relaxation factor by

$$\omega = \frac{2}{1 + \sqrt{1 - r^{(k)}}}. \tag{40}$$

If $m > 1$, omit this calculation.

Increase the value of the outer iteration index by unity, i.e., replace m by (m + 1), and resume successive overrelaxation by returning to step 7.